République Algérienne Démocratique et Populaire

Ministère de l'Enseignement Supérieur et de la Recherche Scientifique

Université d'El-Oued

Faculté de Technologie

Unité de Développement des Energies Renouvelables dans les Zones Arides (UDERZA)

Thèse de Doctorat

Présentée en vue de l'obtention du diplôme de Docteur en Science

Filière: Génie Mécanique

Spécialité: Construction Mécanique

Développement et analyse des performances d'un séchoir solaire intégrant un stockage thermique par chaleur latente

Présenté par: BOUSBIA SALAH Seif Eddine

Soutenue le [Jour/Mois/2025], en présence du Comité de Jury:

ATIA Abdelmalek	Prof.	Université d'El Oued	Président
BENSEDDIK Abdelouahab	Directeur de recherche	URAER de Ghardaïa	Rapporteur
MENECEUR Noureddine	MCA	Université d'El Oued	Co-Rapporteur
BOUKHARI Ali	MCA	Université d'El Oued	Examinateur
DAOUD Djamel	Directeur de recherche	URAER de Ghardaïa	Examinateur
BOUBEKRI Abdelghani	Prof.	Université d'Ouargla	Examinateur

Année universitaire: 2024-2025 / 1446-1447 AH

People's Democratic Republic of Algeria

Ministry of Higher Education and Scientific Research

University of El Oued

Faculty of technology

Renewable Energy Development Unit in Arid Zones (UDERZA)

A Doctoral Thesis

Submitted in Fulfillment of the Requirements for the Degree of Doctor of Science

Field: Mechanical Engineering

Specialization: Mechanical Construction

Development and performance analysis of a solar dryer integrating latent heat thermal storage

Presented by: BOUSBIA SALAH Seif Eddine

Defended on [Day/Month/2025], in the presence of the Jury Committee:

ATIA Abdelmalek	Prof.	University of El Oued	Chair
BENSEDDIK Abdelouahab	Director of research	URAER of Ghardaïa	Supervisor
MENECEUR Noureddine	MCA	University of El Oued	Co-Supervisor
BOUKHARI Ali	MCA	University of El Oued	Examiner
DAOUD Djamel	Director of research	URAER of Ghardaïa	Examiner
BOUBEKRI Abdelghani	Prof.	University of Ouargla	Examiner

Academic Year: 2024-2025 / 1446-1447 AH

Dedications

To my generous parents, God save them.

To my dear wife and our lovely children.

Seif eddine

Acknowledgments

First and foremost, I thank ***ALLAH*** the Almighty and praise Him for granting me the courage, willpower, patience, and success to carry out this work.

I would like to express my deepest gratitude to my thesis supervisor, Professor ***Abdelouahab BENSEDDIK***, for his availability, patience, and trust. I sincerely thank him for guiding my work with great interest and passion, from which I have learned and grown significantly in many areas, both scientific and in terms of writing and organization. His support enabled me to complete my research under highly enriching and satisfying conditions.

I also extend my thanks to the Co-Supervisor, Professor ***Noureddine MENECEUR***, for his assistance and for agreeing to supervise me on this thesis.

My thanks to Professor ***Khaled LOUSSIF***, Head of the Renewable Energy Development Unit in Arid Zones (*UDERZA*) in El-Oued, for kindly welcoming me and facilitating the experimental work for my thesis at the Unit.

A big thank you to the ***members of the jury*** for their time, expertise, and thoughtful evaluation of this thesis. Their comments were essential in refining and strengthening the arguments presented.

My sincere thanks also go to everyone who, directly or indirectly, contributed to the completion of this work, as well as to all those who enriched me with their knowledge. I wish to express my heartfelt gratitude to all of them.

Thesis Abstract

Abstract

This thesis presents the design, development, and performance evaluation of an innovative solar dryer that integrates a parabolic trough collector (PTC), a dual-axis solar tracking system, and a thermal energy storage unit based on phase change materials (PCMs). The system addresses key limitations of traditional solar drying methods, particularly their low efficiency during late afternoon hours and under unstable weather conditions.

Constructed with cost-effective, locally available materials, the prototype was tested under real environmental conditions in El Oued, Algeria. The collector achieved a peak thermal efficiency of 45.25% and maintained drying chamber temperatures up to 70 °C. The integration of PCMs allowed the system to extend drying activity up to four hours after sunset, enhancing energy utilization and system autonomy.

The dryer successfully reduced the moisture content of apricot slices from 69% to 8% (wet basis) and outperformed conventional methods: 65.8% more efficient than shade drying, 50.4% better than open sun drying, and 15.4% more effective than the same system without PCM.

Economic analysis revealed short payback periods (0.36-0.43 years) and annual savings exceeding 3,000 USD, confirming the system's viability for agricultural use. Numerical modeling validated the experimental findings, with strong agreement ($R^2 = 0.97228$, $\chi^2 = 0.21674$). A patent (INAPI No. 241370) was filed to protect the system's design. The study contributes to sustainable solar drying technologies and supports energy transition and food preservation goals in solar-rich regions like Algeria.

Keywords: Solar drying; parabolic trough concentrator (PTC); Dual-axis solar tracking system; Phase change materials (PCM); Thermal energy storage; Energy efficiency; Optical efficiency; Experimental validation; Economic analysis.

Résumé

Cette thèse présente la conception, le développement et l'évaluation des performances d'un séchoir solaire innovant intégrant un concentrateur parabolique cylindro-parabolique (PTC), un système de suivi solaire à deux axes, ainsi qu'une unité de stockage thermique à base de matériaux à changement de phase (PCM). Le système proposé vise à surmonter les principales limites des méthodes traditionnelles de séchage solaire, notamment leur faible rendement durant les fins d'après-midi et sous des conditions climatiques instables.

Fabriqué à partir de matériaux locaux et économiques, le prototype a été testé dans des conditions environnementales réelles à El Oued, en Algérie. Le concentrateur a atteint un rendement thermique maximal de 45,25 % et a permis de maintenir une température de 70 °C dans la chambre de séchage. L'intégration des PCM a permis de prolonger l'activité de séchage jusqu'à quatre heures après le coucher du soleil, améliorant ainsi l'autonomie énergétique du système.

Le séchoir a réduit l'humidité des tranches d'abricot de 69 % à 8 % (base humide) et a surpassé les méthodes classiques : 65,8 % plus efficace que le séchage à l'ombre, 50,4 % plus performant que le séchage à l'air libre, et 15,4 % plus efficace que le même système sans PCM.

L'analyse économique a révélé des périodes de retour sur investissement très courtes (0,36 à 0,43 an) et des économies annuelles dépassant 3 000 USD, confirmant la viabilité du système pour un usage agricole. La modélisation numérique a validé les résultats expérimentaux avec une excellente concordance ($R^2 = 0,97228$, $\chi^2 = 0,21674$). Un brevet (INAPI n° 241370) a été déposé pour protéger le design du système. Cette étude contribue au développement des technologies de séchage solaire durable et soutient les objectifs de transition énergétique et de conservation alimentaire dans les régions riches en soleil comme l'Algérie.

Mots-clés : Séchage solaire ; concentrateur parabolique (PTC) ; système de suivi solaire à deux axes ; matériaux à changement de phase (PCM) ; stockage thermique ; rendement énergétique ; efficacité optique ; validation expérimentale ; analyse économique.

الملخص

تُقدّم هذه الأطروحة تصميم وتطوير وتقييم مجفف شمسي مبتكر يدمج بين مجمّع شمسي ذي قطع مكافئ (PTC) ، ونظام تتبّع شمسي ثنائي المحور، ووحدة لتخزين الطاقة الحرارية تعتمد على مواد تغيير الطور .(PCM) يهدف هذا النظام إلى معالجة أبرز القيود التي تعاني منها طرق التجفيف الشمسي التقليدية، خاصة انخفاض الكفاءة خلال ساعات ما بعد الظهيرة أو في ظل ظروف جوية غير مستقرة. تم تصنيع المجفف باستخدام مواد منخفضة التكلفة واختباره تجريبيا تحت الظروف المناخية الحقيقية في جامعة الوادي، الجزائر.

تم تقييم الأداء الحراري والبصري للنظام بدقة، حيث بلغ الحد الأقصى للكفاءة الحرارية للمجمّع 45.25%، بينما حافظت غرفة التجفيف على درجات حرارة تصل إلى 70 درجة مئوية. ساهم دمج مواد PCM في استمرار عملية التجفيف حتى أربع ساعات بعد غروب الشمس، مما حسّن من استغلال الطاقة وزاد من استقلالية النظام. نجح المجفف في خفض محتوى الرطوبة في شرائح المشمش من 69% إلى 8% (على أساس الوزن الرطب)، وأظهر تحسنًا كبيرًا مقارنة بطرق التجفيف التقليدية: 65.80% مقارنة بالتجفيف في الظل، 50.37% مقارنة بالتجفيف في الهواء الطلق، و15.38% مقارنة بنفس النظام بدون.PCM

أظهر التحليل الاقتصادي فترات استرداد قصيرة جدًا (0.36–0.43 سنة)، ومدخرات سنوية تتجاوز 3000 دولار، مما يؤكد جدوى استخدامه في المجال الزراعي. كما أثبتت النمذجة العددية توافقًا كبيرًا مع النتائج التجريبية (معامل التحديد $R^2 =$ 0.97228، ومربع كاي $\chi^2 = 0.21674$). تم إيداع طلب براءة اختراع لهذا المجفف لدى المعهد الوطني للملكية الصناعية (INAPI) تحت رقم 241370، تأكيدًا على أصالته وقيمته التقنية. تمثل هذه الأطروحة مساهمة علمية وتقنية مهمة في مجال تقنيات التجفيف المستدام، وتدعم أهداف الانتقال الطاقوي والأمن الغذائي في المناطق الغنية بالطاقة الشمسية مثل الجزائر.

الكلمات المفتاحية: التجفيف الشمسي؛ المجمع الشمسي ذو القطع المكافئ (PTC)؛ نظام التتبع الشمسي ثنائي المحور؛ مواد تغيير الطور (PCM)؛ تخزين الطاقة الحرارية؛ الكفاءة الحرارية؛ الكفاءة البصرية؛ التحليل التجريبي؛ التحليل الاقتصادي؛ الطاقات المتجددة.

Table of Contents

Chapter III:
Mathematic Models

Chapter IV:
Experimental Study and Methods

Chapter V:
Results and Discussions

List of Tables

List of Figures

Nomenclature and Indices

Latin

A	Flow cross-section [m^2]
A_a	Aperture surface area [m^2]
AC	Annualized cost of dryers [$]
B_b	Savings per batch for solar dryer [$/kg]
B_d	Savings per day for domestic solar dryer in the jth year [$]
B_j	Annual savings for domestic solar dryer in the jth year [$]
B_{kg}	Savings per kg in comparison to branded product for solar dryer [$/kg]
C	Solar geometrical concentration factor
C_g	Geometric concentration ratio
c_p	Air constant p specific heat capacity [J kg^{-1} $°C^{-1}$]
c_{pl}	PCM Liquid specific heat capacity [J kg^{-1} $°C^{-1}$]
c_{ps}	PCM Solid specific heat capacity [J kg^{-1} $°C^{-1}$]
C_{ac}	Cost of the dryer's components [$]
C_{cd}	Capital cost of solar dryer [$]
C_{ee}	Unit price for electricity [$/kWh]
C_{el}	Cost of electrical energy [$]
C_m	Cost of maintenance [$]
CD_{kg}	Cost of drying per kg of dried product in dryer [$/kg]
C_{drys}	Cost per kg of dried product for domestic solar dryer [$/kg]
C_{dry}	Cost of fresh product per kg of dried product [$/kg]
C_{fre}	Cost per kg of fresh product [$/kg]
D	External diameter of the receiver tube [m]
d_{ext}	External tube diameter of the receiver [m]
d_{int}	Internal tube diameter of the receiver [m]
d_{duct}	Circular duct [m]
D	Inner diameter of the receiver tube [m]
D_h	Hydraulic diameter [m]
D_{eff}	Effective diffusivity coefficient
D_{year}	Number of days of use of domestic dryer per year
f	Focal distance [m]
F'	Collector efficiency factor
F_R	Collector heat removal factor
G_{bn} I_d	Normal beam irradiance [W m^{-2}]
G_{bT} I_G	Normal to aperture area beam irradiance [W m^{-2}]
H	Depth vertical height of the reflector [m]
h_a	Air heat transfer coefficient [W m^{-2} $°C^{-1}$]
h_{fus}	PCM Latent heat of fusion [KJ kg^{-1}]
H_{max}	Maximum height of bearing metal structure[m]
i	Specific enthalpy [J kg^{-1}]

$\boldsymbol{k}$	Thermal conductivity [W m^{-1} °C^{-1}]
$\boldsymbol{k_l}$	PCM Liquid thermal conductivity[W m^{-1} °C^{-1}]
$\boldsymbol{k_s}$	PCM Solid thermal conductivity [W m^{-1} °C^{-1}]
$\boldsymbol{L}$	Length of the receiver tube [m]
$\boldsymbol{L_c}$	Length of the collector mirrors [m]
$\boldsymbol{L_h}$	Characteristic heating length in the receiver tube [m]
$\boldsymbol{L_{ext}}$	External tube length of the receiver [m]
$\boldsymbol{L_{int}}$	Internal tube length of the receiver [m]
$\boldsymbol{\dot{m}}$	Air mass flow rate [kg s^{-1}]
$\boldsymbol{M}$	Mass of PCM [kg]
$\boldsymbol{Mc}$	Initial moisture content on a wet basis
$\boldsymbol{MR}$	Moisture ratio
$\boldsymbol{M_{fre}}$	Mass of fresh product loaded in solar dryer per batch [kg]
$\boldsymbol{M_{dry}}$	Mass of dried product removed from solar dryer per batch [kg]
$\boldsymbol{M_{year}}$	Mass of product dried in the dryer per year [kg]
$\boldsymbol{P}$	Receiver tube cross-section perimeter [m]
$\boldsymbol{P_p}$	Payback period
$\boldsymbol{Pr}$	Prandtl number
$\boldsymbol{\dot{Q}}$	Thermal power [W]
$\boldsymbol{\dot{q}_s}$	Incident concentrated solar irradiance [W m^{-2}]
$\boldsymbol{\dot{q}_u}$	Useful thermal power flux [W m^{-2}]
$\boldsymbol{r}$	Half-thickness of the material sample [m]
$\boldsymbol{Re}$	Reynolds number
$\boldsymbol{R_g}$	Specific gas constant = R/M_g [m^2 s^{-2} °C^{-1}]
$\boldsymbol{S}$	The salvage value[$]
$\boldsymbol{S_a}$	Annualized salvage value [$]
$\boldsymbol{Sl}$	Slenderness parameter
$\boldsymbol{T}$	Temperature [K]
$\boldsymbol{T_m}$	PCM melting temperature [°C]
$\boldsymbol{U_L}$	Thermal losses overall coefficient [W m^{-2} K^{-1}]
$\boldsymbol{\Delta V}$	PCM Volumetric expansion
$\boldsymbol{W_a}$	Rectangular aperture total width [m]
$\boldsymbol{W_p}$	Rated power of electric blower and axial fans [kW]
$\boldsymbol{X_c}$	Initial moisture content on a wet basis
$\boldsymbol{X_0}$	Moisture content (dry basis) at t = 0
$\boldsymbol{X_e}$	Moisture content (dry basis) at equilibrium
$\boldsymbol{X_t}$	Moisture content (dry basis) at time t

Greek

$\boldsymbol{\varphi}$	Extended surface coefficient
ν	Kinematic viscosity
$\boldsymbol{\theta}$	Dimensionless temperature
$\boldsymbol{\gamma}$	Intercept factor
$\boldsymbol{\gamma_e}$	Isentropic exponent
η_{op}	Optical efficiency
η_{th}	Thermal efficiency

Ψ_p	The rim angle [°]
τ	Cover transmittance
α	The absorber absorbance
μ	Dynamic viscosity [$kg \cdot m^{-1} \cdot s^{-1}$]
π	Pressure ratio
ρ	Density [$kg\ m^{-3}$]
ρ_c	Mirror concentrator reflectance
ρ_l	Liquid density of PCM [$kg\ m^{-3}$]
ρ_s	Solid density of PCM [$kg\ m^{-3}$]
$\zeta_{Vertically}$	Vertical rotation aperture angle [°]
$\zeta_{horizontally}$	Horizontal rotation aperture angle [°]

Subscripts

a	Air
amb	Ambient
atm	Atmospheric
c	Compression
e	Expansion
ex	Receiver tube external surface
k	Kinetic energy component
m	Average along the receiver
max	Maximum
min	Minimum
n	Outlet of supply tube to receiver
in	Receiver inlet
ou	Receiver outlet
p	Polytropic, pumping
R	Recirculation, over-pressure
r	Receiver
u	Useful
w	Wall
2	Drying chamber outlet Temperature T_2[°C]
3	Drying chamber inlet Temperature T_3[°C]
4	Receiver air inlet Temperature T_4[°C]
5	Receiver wall Temperature T_5[°C]
6	Receiver air outlet Temperature T_6[°C]

Acronyms

CPTSC	Concentrator Parabolic Trough Solar Collector
CPC	Compound Parabolic Concentrator
FAO	Food and Agriculture Organization of the United Nations
GSA	Global Solar Atlas
HTF	Heat Transfer Fluid
HDH	Humidification and Dehumidification
INAPI	National Institute of Industrial Property
MISD	Mixed-mode Indirect Solar Dryer
NMO	National Meteorological Office
PTC	Parabolic Trough Concentrator

PCM	Phase Change Material
PDC	Parabolic Dish Concentrator
SDPTC	Solar Dryer assisted by a Parabolic Trough Concentrator
SDPTC-PCM	Solar Dryer assisted by a Parabolic Trough Concentrator with PCM
TES	Thermal Energy Storage

Others

⟨ ⟩	Functional dependence
DZD	Local currency
$	US Dollar

General Introduction

General Introduction

Context

In light of the growing challenges related to energy security and climate change, it has become essential to shift towards sustainable and efficient energy solutions, especially in countries with limited conventional energy resources and high import costs. Among these solutions, solar energy stands out as a renewable and clean source that can be harnessed in various applications, most notably in agricultural and industrial drying processes, which represent a fundamental pillar in food and pharmaceutical production chains.

In this context, Algeria is considered one of the richest countries in the world in terms of solar radiation, with annual solar radiation rates ranging from 3 to 5.6 kWh/m² depending on the region, and more than 3,900 hours of solar radiation recorded annually in the Sahara Desert **[1, 2].** According to estimates by the National Agency for the Promotion and Rationalization of Energy Use (APRUE), affiliated with the Ministry of Energy and Mines, Algeria has enormous potential for solar energy production exceeding 14 TWh annually **[3, 4]**. Despite this wealth, the use of solar energy in the agricultural sector remains limited, especially in drying processes, which are often conducted using traditional methods that are costly or ineffective, leading to significant post-harvest losses.

Official data from agricultural authorities indicate that post-harvest production loss in Algeria exceeds 20 to 30% for some products, due to the absence of effective preservation methods such as thermal control or rapid drying **[5]**. These losses are even higher in inland and southern regions, where cooling methods are impractical due to limited energy infrastructure and high temperatures. Therefore, solar drying presents a strategic option to enhance the quality of agricultural products, reduce losses, and improve farmers' income, while also preserving the environment.

Moreover, the development of this technology aligns with Algeria's national energy transition strategy, which aims to achieve 16 GW of renewable energy by 2035 and reduce reliance on natural gas in non-critical sectors **[6]**. Integrating innovative solar drying systems is expected to support this transition, especially in rural areas where they can be locally deployed without the need for complex electrical networks.

Problematic and research objectives

Solar drying technologies, while sustainable and well-suited to sun-rich regions like Algeria, continue to face significant limitations in dynamic and operational performance. Conventional systems are often unable to maintain efficient operation during the late afternoon or under intermittently cloudy skies, leading to inconsistent drying, increased energy losses, and reduced product quality. These shortcomings are largely due to the absence of adaptive mechanisms, particularly solar tracking systems and thermal energy storage units, which are essential for maximizing solar utilization and maintaining thermal continuity.

In addition to the variability of solar radiation, environmental factors such as wind and ambient temperature fluctuations can significantly disrupt the thermal stability of drying chambers, especially in structures made from low-cost or poorly insulated materials. Most existing systems lack the robustness and responsiveness required to sustain efficient drying under such real-world conditions. As a result, post-harvest losses remain high, and adoption of solar drying technology for agricultural use is limited.

This thesis addresses these limitations by developing an innovative solar dryer that integrates three key technological solutions: (1) a dual-axis solar tracking system to optimize solar radiation capture throughout the day, (2) a thermal energy storage unit using phase change materials (PCMs) to extend operation into the evening or during solar intermittence, and (3) a thermally stable, wind-resistant drying chamber designed to maintain consistent internal conditions under fluctuating weather.

The significance of this research lies in its holistic response to the multifaceted challenges of solar drying in Saharan and semi-arid environments. By combining mechanical innovation, material optimization, and energy storage, the proposed system represents a major step forward in the design of autonomous, cost-effective, and high-efficiency solar dryers for rural and semi-urban agricultural contexts.

The main objectives of the study are as follows:

- ✓ To design and construct a solar dryer equipped with a dual-axis tracking system for real-time solar orientation.

- ✓ To develop and integrate a PCM-based thermal storage unit for ensuring continued drying performance after sunset or during cloud cover.
- ✓ To assess the influence of environmental factors such as wind and temperature fluctuations on the thermal stability and performance of the drying system.
- ✓ To evaluate the technical, thermal, and economic performance of the proposed dryer through a combination of experimental tests and numerical simulations under real operating conditions.

Methodology

The methodology of this thesis is structured into distinct chapters, each addressing a specific aspect of the research. A systematic approach was adopted, combining engineering design, numerical simulation, and experimental testing to evaluate the performance of the innovative solar dryer under varying climatic conditions. An in-depth analytical framework was applied to thermal and kinetic data to derive accurate results that support the development of a high-efficiency, stable-performance drying system suitable for practical implementation. Below is an outline of the methodology used in each chapter:

Chapter I presents a comprehensive and systematic review of the relevant scientific literature, with a focus on key studies and the identification of existing knowledge gaps. The review covers the research areas of drying processes, dryer technologies, and solar concentrator systems. Information is meticulously collected, classified, and analyzed to develop a clear and in-depth understanding of the field. The findings are organized and presented using tables, illustrative diagrams, and mind maps to highlight conceptual relationships. Additionally, Bibliometric analysis is employed to support the exploration of research trends and connections, contributing to a well-structured and integrated perspective on the topic.

Chapter II presents the design and construction of the first solar dryer that utilizes concentrated solar radiation through a parabolic trough collector equipped with a dual-axis solar tracking system to generate hot air. The system is capable of maintaining stable temperatures within the desired range suited for drying agricultural products and is supported by a thermal energy storage feature using phase change materials (PCMs). The optical and thermal efficiencies of the solar dryer were also evaluated based on its thermal and geometric parameters. A patent application for this innovation has been filed with the National Institute of Industrial Property (INAPI) under registration number 241370.

Chapter III presents the mathematical models contained in this thesis:

- The development and validation of numerical models to simulate solar drying systems. Both mathematical and physical modeling approaches are used to evaluate the performance of the developed solar drying system. This process has helped in understanding how key design and operational variables such as solar irradiance, air mass flow rate, and geometric concentration affect the outlet air temperature of the solar receiver.
- Next, mathematical modeling equations for drying kinetics are presented, aiming to predict the moisture removal behavior of agricultural products under different thermal conditions.
- Finally, the mathematical formulations required to perform an economic analysis are introduced to evaluate the financial feasibility and cost-effectiveness of the proposed system, taking into account both investment and operating costs. Collectively, these analyses contribute to providing a comprehensive view of the system's technical and economic performance.

Chapter IV presents the experimental setup, with tests carried out in a sunny outdoor area near the Mechanical Engineering Laboratory at El-Oued University, in collaboration with the Renewable Energy Development Unit in Arid Zones (UDERZA). The chapter also explores the meteorological and climatic characteristics, assesses the solar energy potential, and examines the oasis–desert interactions specific to the El Oued study area. The experimental work focuses on evaluating and enhancing the performance of the innovative solar dryer in four main areas:

- Evaluating the performance of the solar dryer under real and typical operating conditions.
- Improving the solar dryer by studying the effect of integrating thermal energy storage using Phase Change Materials (PCM) on thermal performance.
- Assessing the ability of the PCM-enhanced solar dryer to overcome fluctuating natural weather conditions.
- Conducting a comparative analysis of the drying process across different cases: using the innovative solar dryer, the PCM-enhanced solar dryer, in shaded conditions, and under direct sunlight.

The experimental procedures include measuring temperature, solar radiation intensity, wind speed, and airflow velocity, in addition to monitoring drying rates and moisture content. The drying performance of the modified solar dryers is compared under both stable and fluctuating climatic conditions.

Chapter V presents the results and discussions related to the work conducted in this thesis. It evaluates and analyzes the performance of the innovative solar dryer through a series of field experiments in a desert environment. The assessment focuses on four main aspects: the dryer's performance under real operating conditions, the impact of integrating Phase Change Materials (PCM) on thermal efficiency, the system's ability to operate under fluctuating weather conditions, and a comparative analysis of drying effectiveness under different scenarios (with PCM, without PCM, in the shade, and under direct sunlight). Additionally, the chapter includes an economic analysis that demonstrates the system's financial viability, confirming its technical effectiveness and cost-efficiency for agricultural solar drying.

Chapter I

Literature Review

Chapter I:

Literature Review

I.1. Introduction

This chapter aims to review the relevant scientific literature by highlighting the most significant previous research efforts and identifying existing knowledge gaps, thereby guiding the current study toward making a valuable scientific contribution. It provides a comprehensive literature review covering most aspects of the thesis research field through the systematic collection, classification, and summarization of various types of information relevant to the topic. The data is presented in a well-organized manner using tables, illustrative diagrams, and mind maps, to facilitate a clear understanding of the relationships between concepts, extract key scientific insights, and reinforce the research direction of the thesis through a structured and integrated approach.

I.2. Basic concepts and theoretical principles

I.2.1. Principles and operation of solar dryers

I.2.1.1. Principles of drying processes

Moisture content, defined as the ratio of a material's water content to its dry weight, is a critical parameter in drying processes and is typically expressed as a percentage. Precise control of moisture content is essential to ensure the stability and quality of dried products. The drying process itself is commonly described using a drying rate curve, which includes two key phases: the constant rate period, during which surface moisture evaporates at a steady rate influenced by external conditions like temperature and airflow; and the falling rate period, where moisture migration from the interior to the surface slows the drying process. The primary mechanisms responsible for moisture removal are evaporation, where liquid water transforms into vapor and is carried away by airflow, and diffusion, which involves the movement of water molecules from areas of higher concentration to lower concentration within the material until they reach the surface and evaporate. Several factors significantly influence the efficiency of the drying process, such as temperature, humidity, airflow, and the physical and chemical properties of the material itself. Higher temperatures enhance evaporation, low humidity accelerates drying by increasing the moisture gradient, and effective airflow facilitates moisture removal. Additionally, material characteristics like porosity and hygroscopicity play a vital role in the overall drying performance **[7, 8].**

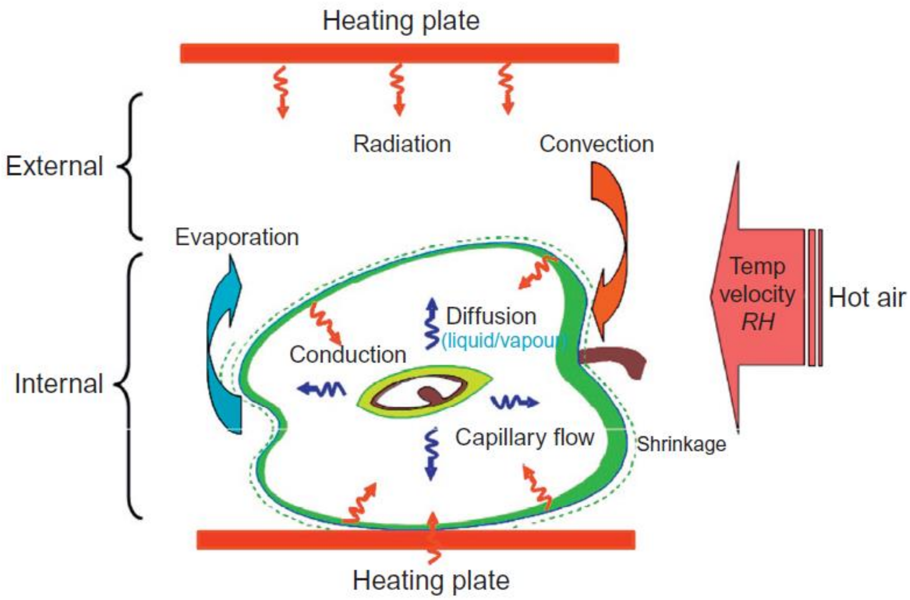

Fig. I.1. Conceptual Schematic of the thermal drying process in solid food materials **[7].**

Drying food materials is a highly complex process that involves simultaneous and transient mechanisms of heat, mass, and momentum transfer, along with associated physical, chemical, and phase change transformations. During this process, two primary transport mechanisms occur concurrently: the transfer of heat from the drying medium or heat source to the food material, and the movement of moisture from within the solid product to its surface. Once at the surface, the moisture is removed either by a carrier gas or through vacuum application in the case of non-convective dryers. These coupled transport phenomena are conceptually represented in Figure.I.1 **[7].**

I.4. State of the art

Numerous empirical studies have explored the use of solar concentrators combined with air as the heat transfer fluid, uncovering several key findings.

A study by **Zhao et al. [29]** investigated how different receiver tube designs in a parabolic trough solar air collector affected its performance. They found that both solar radiation and the design of the receiver tube played a significant role in determining the air temperature the collector could achieve. Tubes with internal pin fins proved to be the most efficient at collecting heat, reaching a temperature of 266°C. In contrast, smooth tubes without these fins could only reach 166°C, highlighting the importance of design in maximizing heat collection **(Figure I.14).**

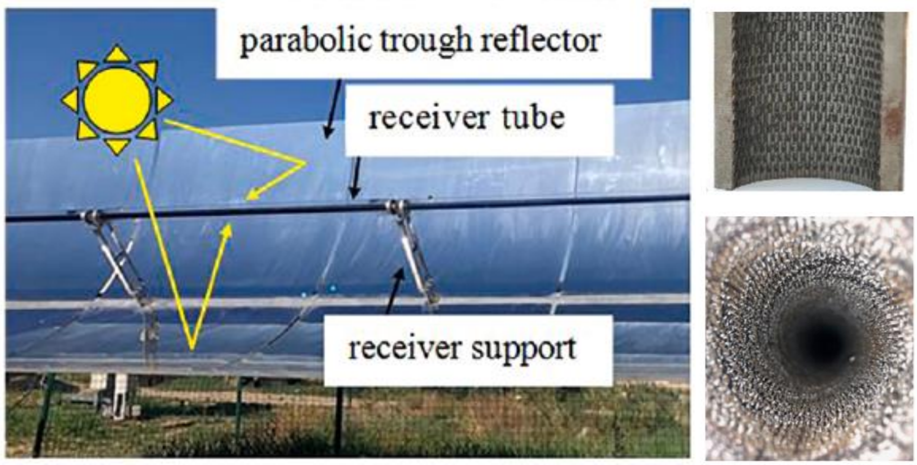

Fig. I.14: A view of a PTAC with an IPF-Tube **[29].**

Nasir [30] Conducted experiments on a parabolic trough solar air heater, a device that uses sunlight to heat air. The results showed that the heater could reach a maximum temperature of 97°C and operated with a respectable 65% efficiency in converting sunlight to heat.

Pandey et al. [31] experimented with a solar heater that used a compound parabolic concentrator to focus sunlight onto an evacuated tube receiver connected to a U-shaped copper pipe. This system was able to achieve a maximum temperature of 151°C while operating at a thermal efficiency of 24.1%, meaning it converted almost a quarter of the sunlight it received into usable heat **(Figure I.15).**

Wang et al. [32] conducted experiments using an all-glass evacuated tube solar air heater integrated with a simplified compound parabolic concentrator. The system successfully achieved air temperatures exceeding 200°C, highlighting its potential for high-temperature air heating applications (**Figure I.16**).

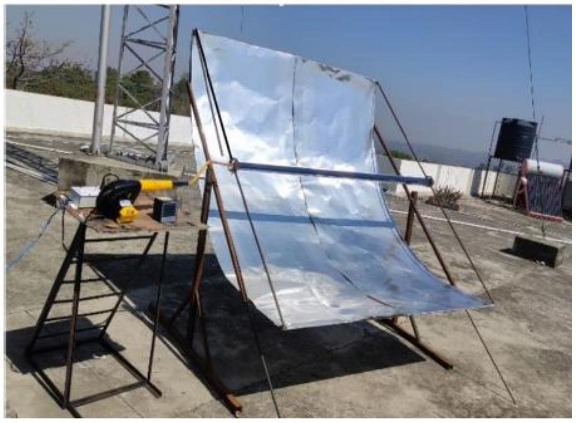

Fig. I.15: PTC with U-shaped copper pipe **[31].**

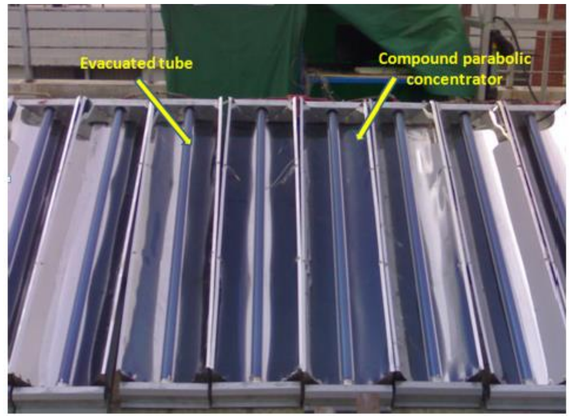

Fig. I.16: solar air heater CPC **[32].**

Good et al. [33] employed air as the heat transfer fluid in a pilot-scale solar power plant, replacing thermal oil to address the temperature limitations associated with oil-based parabolic trough receivers.

Fahad et al. [34] analyzed a humidification-dehumidification (HDH) system that utilized a parabolic trough collector with air as the heat transfer fluid. Their findings indicated an average collector efficiency of 71% and an outlet air temperature of 75°C, demonstrating the system's effectiveness for solar-powered desalination applications.

Karoua et al. [35] combined two solar technologies, concentrated solar power and a flat plate collector, into a single solar air heater using a Linear Fresnel Reflector. The system achieved air temperatures ranging from 70°C to 150°C, highlighting its capability for medium-temperature thermal applications (**Figure I.17**).

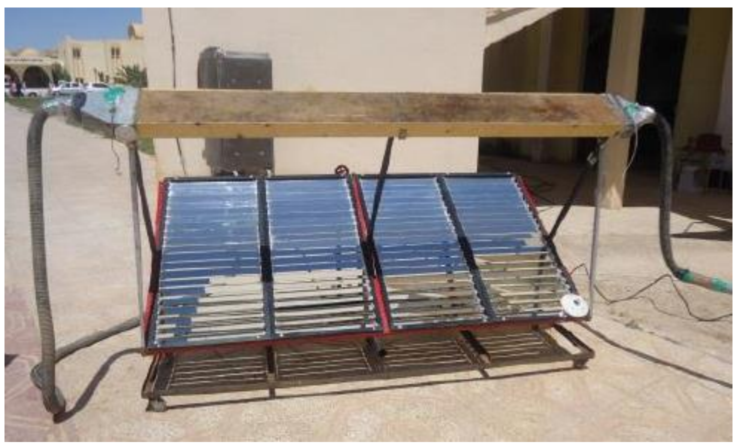

Fig. I.17: Linear Fresnel Reflector (SAHLFR) solar air heater with a rectangular duct absorber **[35].**

Hongfei et al. [36] tested the efficiency of a multi-surface trough solar concentrator under actual weather conditions, and an efficiency of over 45% was achieved (**Figure I.18).**

Fig. I.18: Air heating using a multi-surface trough solar concentrator **[36].**

Chu et al. [37] developed and tested a pressurized air receiver integrated with a concentrated solar dish system. The receiver featured an innovative design with double spiral tubes arranged in a conical configuration. Under direct normal irradiation of around 651 W/m² and a mass flow rate of 0.0048 kg/s, the system achieved an outlet air temperature of 787°C, produced a power output of 3.96 kW, and reached a thermal efficiency of 53.16%.

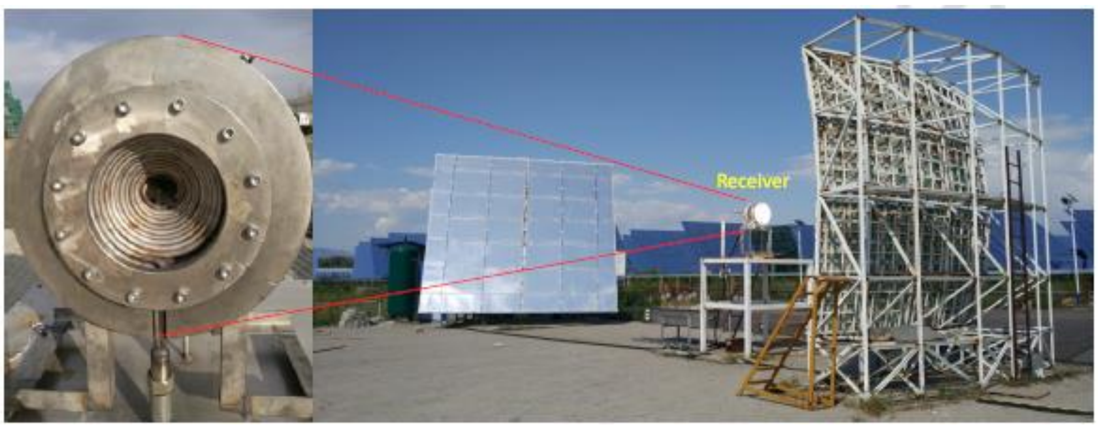

Fig. I.19: Tubular air receiver in solar dish system **[37].**

While existing research showcases the potential of solar air heating systems across various applications like space heating, drying, and desalination, most designs operate at temperatures far exceeding those suitable for delicate processes like agricultural drying. This discrepancy arises despite their use of air as a heat transfer fluid (HTF). The limited scientific literature on air heating using parabolic trough collectors or similar concentrating technologies for drying applications further underscores this gap. The experimental studies mentioned will delve into these specific areas **(Figure I.19).**

We mention these experimental studies: **Laouini et al. [38]** conducted a study employing a solar Parabolic Dish Concentrator (PDC) as the heat source for drying red chili peppers. It's important to note that while the conversion unit receiver reached temperatures as high as 510°C, the temperature within the drying chamber itself remained significantly lower, reaching a maximum of 55°C (**Figure I.20).**

Fig. I.20: Solar Parabolic Dish Concentrator (PDC) for drying **[38].**

Aamir et al. [39] developed and tested a small-scale Concentrating Parabolic Trough Solar Collector (CPTSC) prototype specifically designed for drying applications. They evaluated the CPTSC's performance using two different mass air flow rates, carefully measuring the inlet and outlet air temperatures. Their findings showed that while the absorber tube within the CPTSC reached a maximum temperature of 140°C, the drying chamber itself maintained a significantly lower temperature, peaking at 60°C (**Figure I.21).**

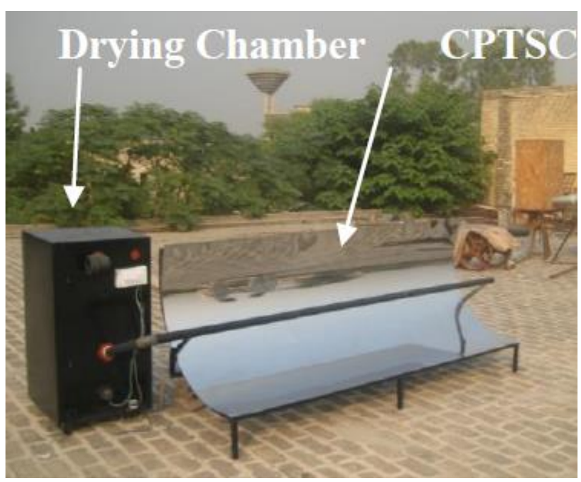

Fig. I.21: Small-scale Concentrating Parabolic Trough for Drying **[39].**

Fahim et al. [40] investigated the influence of airflow rate on both apple drying efficiency and the overall performance of a parabolic trough solar collector. During their study, peak solar irradiation reached 752 $kJ.m^{-2}.hr^{-1}$, coinciding with a maximum ambient temperature of 43°C at noon. Under these peak conditions, with the highest airflow rates, the drying chamber reached 51°C while the absorber pipe within the collector reached 84°C.

In addition, **Fahim Ullah et al. [41]** examined the effectiveness of a Parabolic Trough Solar Concentrator (PTSC) for dehydrating guavas. Their research demonstrated successful drying at a controlled temperature of 65°C and a humidity level of 25%, with a total drying time of 19 hours. Based on their findings, they recommended the PTSC as a viable option for drying various fruits and vegetables, suggesting a potential operating time of up to 9 hours per day.

Chapter II

Design, Construction, and Performance of a New Solar Dryer

Chapter II:

Design, Construction, and Performance of a New Solar Dryer

II.1. Introduction

Based on the content presented in chapter one, covering the review of previous studies, bibliometric analysis, and the identification of research gaps, this chapter introduces the innovative design and construction of the first solar dryer that generates hot air through concentrated solar radiation using a parabolic trough concentrator equipped with a dual-axis solar tracking system. The unique engineering features of this system have enabled the achievement of high optical performance and stable and appropriate temperatures within the thermal range of 40–80 °C, making it highly effective and suitable for drying a wide variety of agricultural products. It is worth noting that a patent application for this solar dryer has been filed with the National Institute of Industrial Property (INAPI) under registration number 241370, affirming the originality and technical value of the innovation.

II.2. Design of prototype solar dryer with PTC system

As part of the preliminary design process, a 3D model along with the engineering projections of the new solar dryer prototype including front, side, and top views was developed using *SolidWorks*. These technical drawings provided an accurate representation of the structural components and facilitated the visualization of the overall system assembly. The use of *SolidWorks* enabled precise dimensional planning and played a pivotal role in optimizing the dryer's design before fabrication.

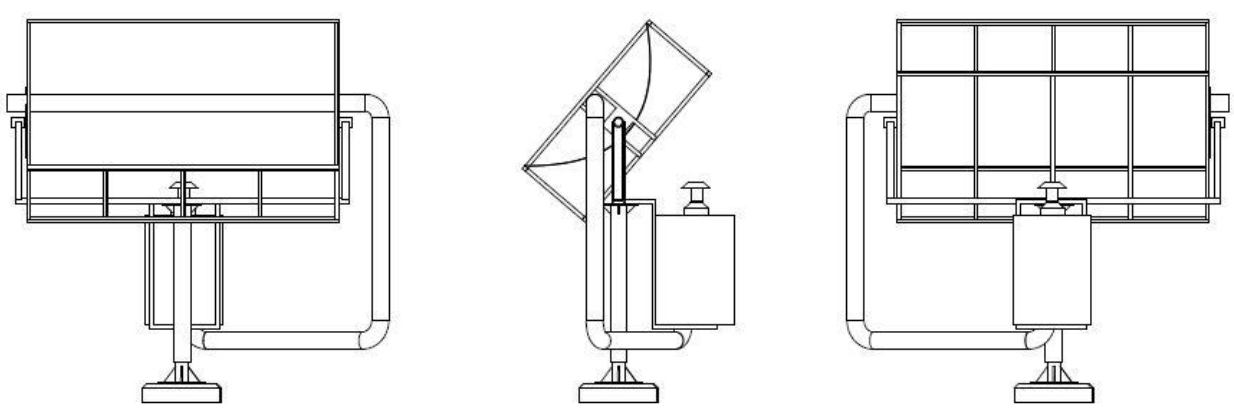

Fig. II.1. Drawing the 3D model and geometric projections of the new solar dryer prototype

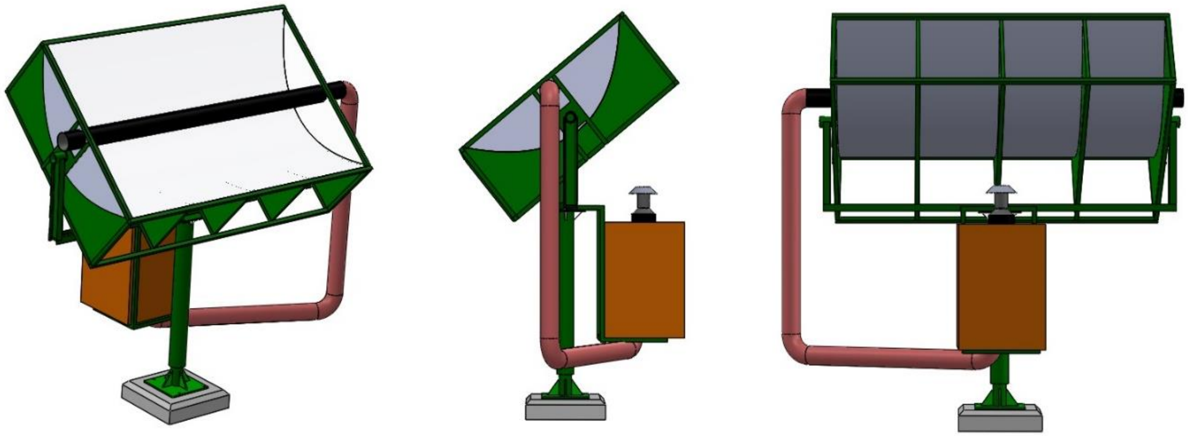

Fig. II.2. The projection views of the new solar dryer prototype were designed using SolidWorks

II.3. Construction of prototype solar dryer with PTC system

II.3.1. Description of the different parts of the prototype

The experimental installation consists of an indirect solar dryer operating under forced load. The schematic diagrams and photographs presented in Figures II.5 and II.6 illustrate the design and geometric dimensions of the solar dryer, along with its main components, which include: (i) a Parabolic Trough Concentrator (PTC), (ii) a receiver tube, (iii) a drying chamber, (iv) a dual-axis solar tracking mechanism, (v) a bearing metal structure, and (vi) a concrete foundation.

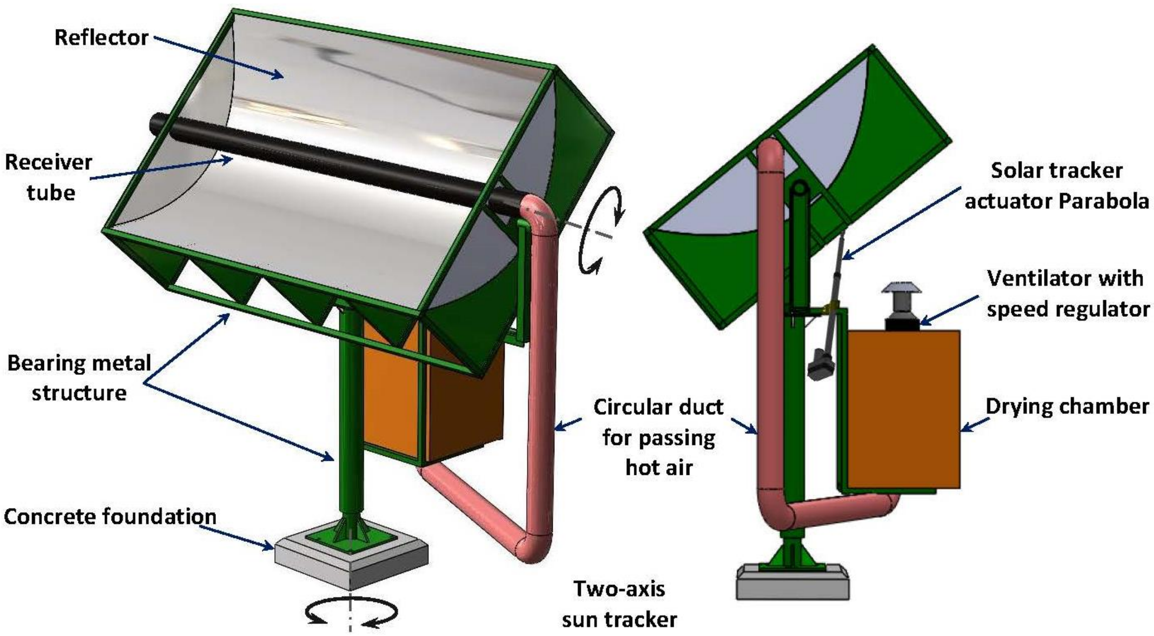

Fig. II.5. The Solar dryer prototype designed using SolidWorks

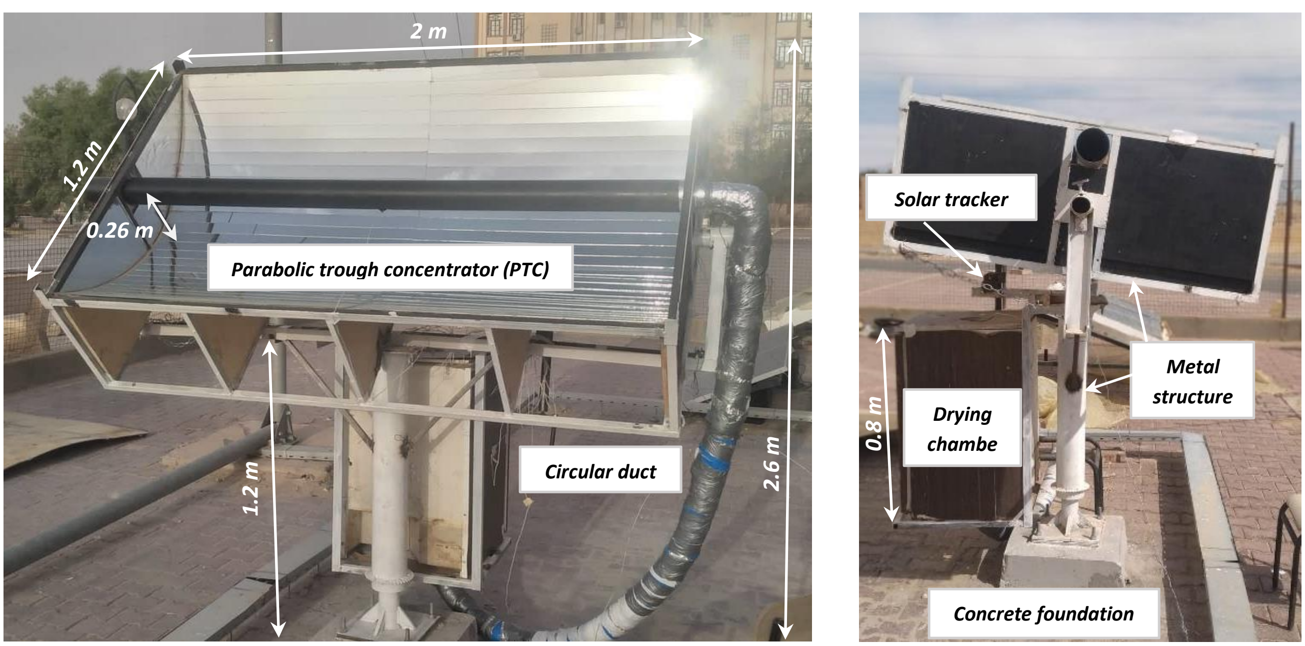

Fig. II.6. General View and geometrical dimensions of a solar dryer assisted by (PTC) made at the University of El Oued

II.3.1.1. Reflector

The solar Parabolic Trough Concentrator (PTC) employed in the experiment features an aperture width of 1.2 m, with a reflector measuring 2 m in length, 0.34 m in depth, and a focal length of 0.2647 m. The total reflective surface area amounts to 2.84 m^2. This surface is covered with small rectangular segments of standard mirrors, each measuring 1 m in length and 0.05 m in width, arranged along the aperture. These mirrors are designed to reflect direct solar radiation onto the receiver, thereby enhancing the overall efficiency of the solar dryer.

Table II.1. Geometric characteristics of the reflector

Geometric characteristics	value
Diameter	W_a =1.2 m
Size	h =0.34 m
Focal distance	f =0.2647 m
The rim angle	Ψ_p = 82.84°
Aperture area	A_a =2.4 m^2

Before initiating the construction phase, the sizing of the solar concentrator was carried out to determine its various geometric parameters. A parabolic arc was generated using the Parabola Calculator 2.0 software, as illustrated in Figure II.7.

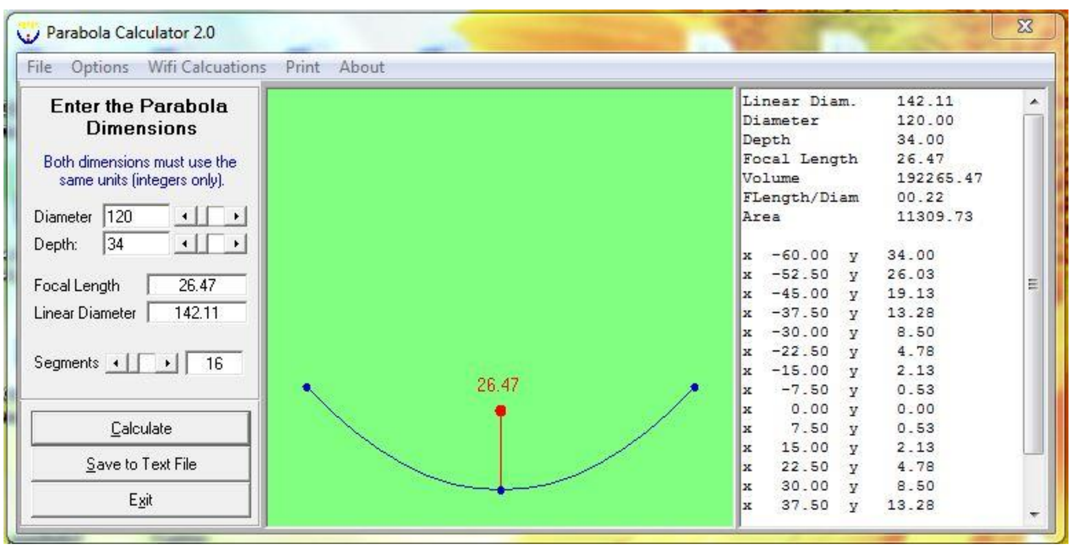

Fig. II.7. Parabola calculator 2.0 software interface

To select an appropriate parabolic-cylindrical reflector, it is recommended to adopt an ideal geometric profile to achieve effective geometric concentration, as illustrated in Figure II.7. A high-quality reflector can reflect up to 97% of the incident solar radiation. The design of the reflector is based on the standard parabolic equation **[58, 59, 60]**. In Cartesian coordinates, the general equation of the reflector is expressed as:

$$x^2 = 4fy \tag{1}$$

And Focal distance:

$$f = \frac{W_a^2}{16h} \tag{2}$$

The rim angle, Ψp, which is directly related to the arc length of the concentrator, can be determined using Eq. (3) as a function of the focal distance *f* of the parabola and the aperture width Wa **[61]**:

$$\tan \Psi p = \frac{8.f.\text{Wa}}{\text{Wa}^2 - 16f^2} \tag{3}$$

II.3.1.2. Receiver

The receiver tube is made of galvanized steel with a thermal conductivity of 50 W/m·K. It has a large diameter of 10 cm, which allows for efficient airflow, a wall thickness of 1 mm, and a total length of 2.2 meters. The tube is installed without a glass cover and positioned at the focal area of the reflector to effectively absorb concentrated solar radiation and convert it into heat. To enhance its solar absorption capabilities, the tube is coated with a thin layer of matte black paint. It features two openings that facilitate airflow: cold ambient air enters through the inlet and passes through the receiver tube, where it is heated before continuing toward the drying chamber.

Table II.2. Geometric characteristics of the receiver

Geometric characteristics	value
Diameter	d = 0.1 m
Size	L = 2 m in concentrator
Receiver area	A_r =0.6283 m^2
Geometric concentration ratio	C_g = 3.82

The geometric concentration ratio, C_g is defined as the ratio of the collector's aperture area A_a to the total surface area of the receiver tube A_r, It is expressed by Eq. (4) as follows **[58, 61, 62, 63]**:

$$C_g = \frac{A_a}{A_r} = \frac{\text{Wa}}{\pi.d} = 3.82 \tag{4}$$

II.3.1.3. Drying chamber

The drying chamber is constructed using sandwich panels insulated with polyethylene foam, which has a low thermal conductivity of approximately 0.039 W/m·K and a thickness of 3 cm. This insulation helps retain hot air within the chamber and minimizes heat loss. Heated air enters the chamber through an opening at the bottom, while humid air is expelled through an exhaust opening at the top, assisted by a ventilator equipped with a speed regulator to enhance airflow. The chamber measures 0.5 m × 0.5 m × 0.8 m and includes multiple levels for sample placement during drying.

The ventilator plays a key role in maintaining air circulation at a flow rate of 2.45 m/s, guiding air from the receiver tube through an insulated connecting duct into the drying chamber (Figure II.10).

II.3.1.4. Support structure

The support structure of this model is composed of three main mechanical assemblies: a metal frame to hold the parabolic reflector, a rotating cylindrical metal column, and a metal stand for the drying chamber. The entire assembly is anchored on a reinforced concrete base embedded 1.2 meters deep into the ground, providing stability during rotation and sufficient strength to support the weight of all components. The design of the structure offers several functional advantages, including:

- Support for the drying chamber in its designated position, allowing it to rotate along with the entire system without obstructing the movement of the reflector.
- Carrying and framing the solar parabolic trough concentrator, enabling smooth rotation along two axes vertically with a full aperture angle of 360°, and horizontally with a range of 250°. This dual-axis movement, in combination with the tracking mechanism, ensures efficient solar tracking throughout the day. It combines the benefits of a sensitive mono-axis tracker with enhanced precision, improving performance particularly during seasonal variations and shifts in the sun's inclination angle between summer and winter.

II.3.2. The different steps of prototype realization and construction

The construction of the solar dryer involves several sequential steps. Initially, a reinforced concrete foundation is built, serving as the base for the entire system. This foundation has a depth of 0.8 meters and a width of 0.5 meters, providing stability for the overlying metal structure.

.

(a) (b) (c) (d)

Fig. II.8. (a, b, c, d). The various stages of building a concrete foundation

The next step includes welding the metal framework according to the planned design, followed by the use of a lathe machine to install a tapered roller bearing to enable smooth rotation. Finally, the different components of the system such as the parabolic trough concentrator, receiver tube, and drying chamber are assembled onto the structure. These steps are illustrated in Figures II.8 and II.9.

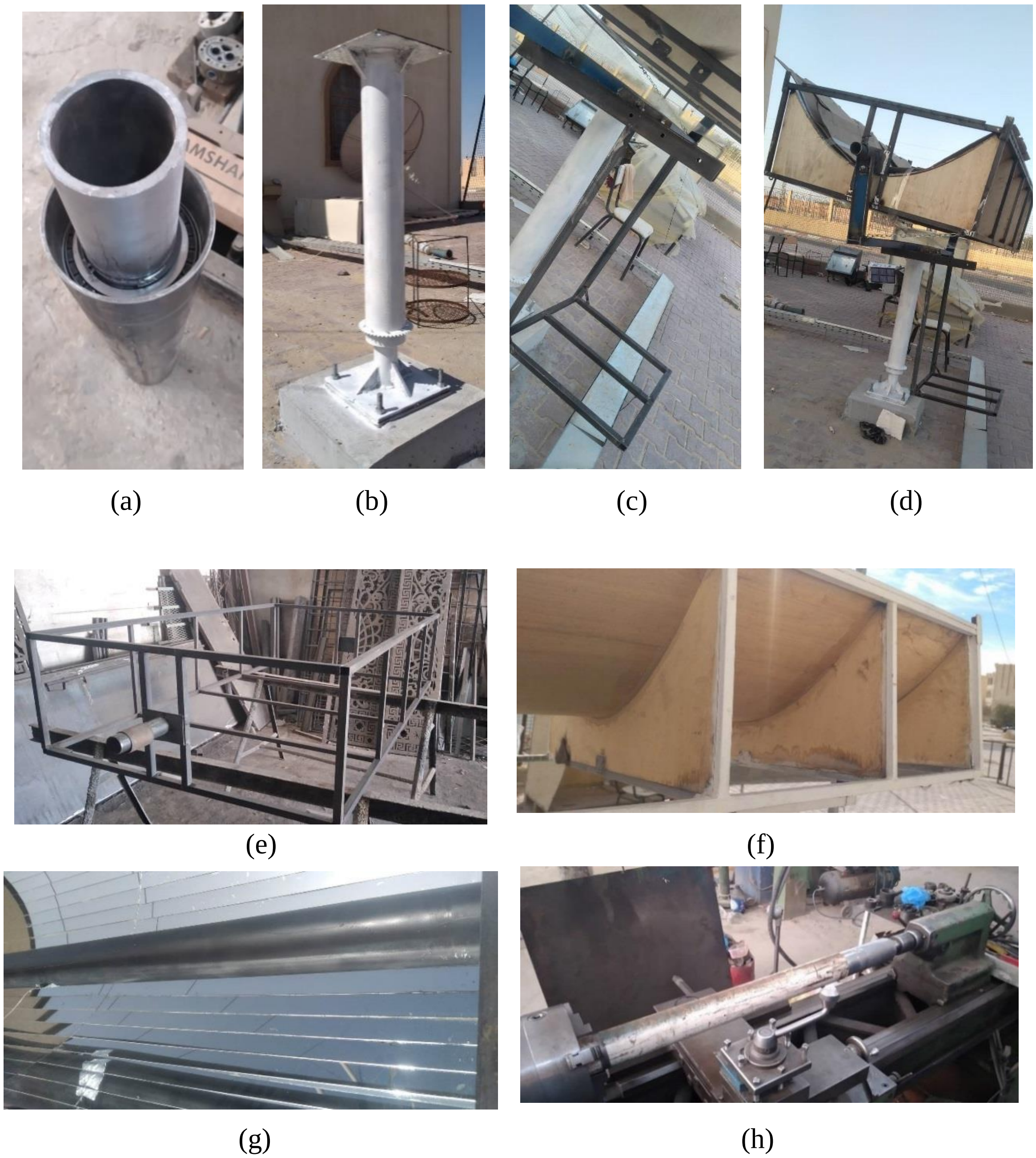

Fig. II.9. The various components of the support structure: (a, b, h) metal rotary cylindrical column with two tapered rollers bearings using the lathing machine, (e, f) metal Frame incubator for a reflector, (g) reflector mirror, (c, d) metal stand for a drying chamber

II.4. Performance of Parabolic Trough Concentrator (PTC) of the solar dryer

The performance analysis characterizes the solar field under various operating conditions for the system being studied. The key performance indicators considered in this analysis are the solar field efficiency and the useful thermal energy output generated by the solar field.

II.4. 1. Optical Performance

The optical efficiency, (η_{opt}) is defined as the ratio of radiation absorbed by the absorber tube to the amount of direct typical radiation incident on the aperture area. When the incidence angle of the solar flux onto the PTC aperture plane is 0° gives the peak optical efficiency in Eq (5) **[58, 64]:**

$$\eta_{opt} = \rho_c \times \gamma \times \tau \times \alpha \tag{5}$$

The optical efficiency (η_{opt}) is the multiplication of the mirror reflectance ρ_c, the intercept factor γ, the glass transmittance τ, and the absorber absorptance α **[65].**

The optical efficiency is influenced by both the optical properties of the materials used and the geometry of the collector. Properties such as reflectivity, transmissivity, and absorptivity can be experimentally measured in the laboratory. Additionally, the intercept factor, a purely geometric parameter, represents the proportion of solar radiation reflected by the concentrator that is successfully intercepted by the absorber tube, reflecting the overall geometric precision of the system.

Table II.3. The optical efficiency and the optical properties of the materials involved in the geometry of the PTC.

Parameters	Value
optical efficiency (η_{opt})	0.8112
the absorber absorbance (α)	0.94
concentrator reflectance (ρ)	0.938
cover transmittance (τ)	1 without a glass cover
intercept factor (γ)	0.92

II.4. 2. Thermal efficiency

The thermal efficiency (η_{th}) is the ratio of the useful output Q_u [W] delivered by the collector to the global irradiance I_b [W/m^2] incident on the collector aperture area Aa [m^2], to calculate the thermal efficiency of the air heater the following expression is used Eq (6) **[31, 58,61, 64]**:

$$\eta_{th} = \frac{Q_u}{A_a * I_b} = \frac{\dot{m}.C_p\,.\Delta T}{A_a * I_b} \tag{6}$$

The parameters in Table II.4 are used to monitor the variation in thermal efficiency throughout the day.

$\dot{m} = \rho.A.v$ = (1.146). ($0.04^2.\pi$). (2.45)=0.0141 kg/s

$$\eta_{th} = 5.904375.\frac{\Delta T}{I_b}$$

Table II.4. The thermal efficiency changes with time during the day, thermal parameters, and the geometry of the PTC.

Parameters	**Value**
thermal efficiency (η_{th})	Variable in time
the mass flow rate of air ($\dot{m}$)	0.0141 kg/s
the specific heat of the air (C_p)	1005 J/kg-K
the temperature difference between inlet and outlet air (ΔT)	°C Variable in time
the aperture area (A_a)	2.4 m^2
the global solar radiation (I_b)	W/m^2 Variable in time

The thermal efficiency of the system depends on the temperature difference (ΔT) and the beam solar irradiance (I_b), as these factors fluctuate while other parameters are held constant. The average thermal efficiency (ηth) recorded during the experiment is 25.93%, with a maximum observed thermal efficiency reaching 45.25%.

II.6. Conclusion

In conclusion, this chapter presented the innovative design and engineering construction of a prototype solar dryer. The work included the development of a 3D model and technical projections using SolidWorks, which enabled an accurate visualization of the system's components prior to fabrication. The prototype was then built following a well-defined series of implementation steps. A detailed description of the various parts of the solar dryer was provided, including the solar collector, receiver tube, drying chamber, and air circulation system. The geometric characteristics of each component were also described in terms of dimensions, materials used, and the rationale behind their selection. These features collectively contributed to achieving effective solar radiation concentration and thermal stability within the target temperature range of 40–70 °C. The optical and thermal efficiencies demonstrated the system's effectiveness in converting solar energy into heat suitable for drying various agricultural products.

Chapter III

Mathematatic Models

Chapter III:
Mathematic Models

III.1. Introduction

This chapter presents the mathematical models employed in this thesis to analyze and evaluate the performance of the developed solar drying system from both technical and economic perspectives. It begins with the development and validation of numerical models using both mathematical and physical modeling approaches. These models are used to simulate the behavior of the solar drying system and to study the influence of key design and operational parameters such as solar irradiance, air mass flow rate, and geometric concentration on the outlet air temperature of the solar receiver. Subsequently, mathematical models related to drying kinetics are introduced, aiming to predict the moisture removal behavior of agricultural products under various thermal conditions. These models help in improving drying efficiency and adapting the system to changing climatic conditions. Finally, the chapter presents the mathematical formulations used for economic analysis, which evaluate the financial feasibility and cost-effectiveness of the proposed system by considering both investment and operating costs. Together, these models provide a comprehensive framework for assessing the overall technical and economic performance of the solar drying system.

III.2. Effect of basic parameters on the outlet air temperature of the receiver

This section employs a simplified 1D analysis to establish a foundational framework for evaluating the studied concept, as outlined in **[66].**

Linear concentrating collectors are typically arranged in rows, aligning multiple modules along their axis to achieve a total length, denoted as L_c. The cumulative mass flow rate is distributed among several parallel rows. Each row consists of a rectangular mirror with a length L_c and an aperture area W_a. The solar normal irradiance's beam fraction, denoted as G_{bn}, impacting the mirror aperture width Wa, is concentrated on the tube perimeter Pex. This concentration results in a focused irradiance on the external surface of the receiver tube, denoted as $\dot{q}_s$ (Equation 7), determined by the optical efficiency (η_{op}) and geometric concentration (C).

$$A_a = L_c W_a \, ; \, \dot{q}_s = G_{bn} \eta_{op} C \, ; \, C = W_a / P_{ex} \tag{7}$$

The circular receiver tube, with a diameter D, has an external perimeter P_{ex} and an internal wet perimeter P, reduced due to a wall thickness ew. The contact surface extension factor phi (ϕ)

considers thin internal longitudinal fins, maintaining the cross-section A without significant reduction. The hydraulic diameter D_h decreases as the fin thickness is considered negligible. Thus, the cross-section parameters are defined in Equation (8).

$$P_{ex} = \pi(D + 2e_w)\ ;\ P = \varphi\pi D\ ;\ A = \pi D^2/4\ ;\ D_h = \frac{4A}{P} = D/\varphi \tag{8}$$

In the absence of internal longitudinal fins, the contact surface extension factor φ is equal to 1.

Equation (9) formulates the heat balance at any cross-section of the receiver tube, where UL is the local heat transfer coefficient determining heat losses, T_w is the temperature of the external wall, and T_{amb} is the ambient temperature.

$$\dot{q}_s - U_L(T_w - T_{amb}) = \dot{q}_u \tag{9}$$

The heat transfer coefficient *UL* depends on the geometry of the coaxial tubes and materials, slightly increasing with T_w. For simplicity, *UL* is considered constant with typical values in the literature (*UL* = 3 to 6 W m^{-2} °C^{-1}) **[66]**. In this analysis, *UL* is set to 3 W m^{-2} °C^{-1}. The net heat flux $\dot{q}_u$ is transferred from the wall at temperature T_w to the inner flow at bulk temperature T, linked by the heat transfer coefficient of the inner air h_a (Equation 10).

$$\dot{q}_u = \frac{h_a P(T_w - T)}{P_{ex}} \tag{10}$$

The heat transfer coefficient h_a is expressed by the Dittus-Boelter correlation (Equation 11), where Re_D_h is the Reynolds number, Pr is the Prandtl number, and $\dot{m}$ represents the mass flow rate.

$$h_a = \frac{k}{D_h} 0.023 Re_{D_h}^{0.8} Pr^{0.4}\ ;\ Re_{D_h} = \frac{4\dot{m}}{\mu\pi D\varphi} \tag{11}$$

The fluid (air) properties, including specific heat, dynamic viscosity, thermal conductivity, and density (all temperature-dependent properties), are calculated using Equation (12) **[67, 68]**:

$$C_p = (1.1788 - 2.8765 * 10^{-3}T + 1.8105 \times 10^{-5}T^2 - 5.1000 \times 10^{-8}T^3 + 5.4000 \times 10^{-11}T^4) * 1000 \tag{12}$$

$$\mu = 3.2575 \times 10^{-5} - 7.56163 \times 10^{-7}T + 7.47253 \times 10^{-9}T^2 - 2.86507 \times 10^{-11}T^3 + 3.89067 \times 10^{-14}T^4 \tag{13}$$

$$k = -3.06000 \times 10^{-4} + 9.89089 \times 10^{-5}T - 3.46571 \times 10^{-8}T^2 \tag{14}$$

$$\rho = \frac{P_{atm}}{RT} \tag{15}$$

The specific gas constant: $R = 287$ (J/kg K) and $P_{atm} = 101325\ P_a$. Here, T represents the absolute air temperature in Kelvin.

The 1D model leads to the determination of the total solar heat power $\dot{Q}_u$ (Equation 16), expressed in terms of T_{in}, T_{out}, and T_{amb} (Equations 17 and 18). Equation (19) introduces the collector efficiency factor *F'*, using Equation (11) to obtain the last term. Equation (20) illustrates the origin of the heat dissipation factor F_R **[66]**, relying on constant U_L, h_a, $\dot{q}_s$, and fluid properties, along L.

$$\dot{Q}_u = P_{ex} \int_0^L \dot{q}_u dx \tag{16}$$

$$\dot{Q}_u = F_R L P_{ex}[\dot{q}_s - U_L(T_{in} - T_{amb})] = \dot{m}(i_{out} - i_{int}) \tag{17}$$

In line with current practices, enthalpy is approximated using a temperature-varying C_p, allowing the explicit representation of pressures and temperatures in turbomachines and solar collectors (Equation 18).

$$\dot{Q}_u = \dot{m}(i_{out} - i_{int}) \cong \dot{m}(C_{p,ou}T_{out} - C_{p,in}T_{int}) \tag{18}$$

The connection between wall and flow temperature is given by the collector efficiency factor *F'* (Equation 19), considering $P_{ex} > P$. Equation (20) provides an analytical expression of $F_R$by integrating temperature from the tube inlet ($x = 0, T = T_{in}$) to the outlet ($x = L, T = T_{out}$), using an average specific heat $C_{p,m}$.

$$F'\langle\dot{m}\rangle = \frac{\dot{q}_s - U_L(T_w - T_{amb})}{\dot{q}_s - U_L(T - T_{amb})} = \left[1 + \frac{U_L P_{ex}}{h_a\langle\dot{m}\rangle P}\right]^{-1} \tag{19}$$

$$F'\langle\dot{m}\rangle P_{ex} dx = \frac{\dot{m} C_{p,m} dT_t}{[\dot{q}_s - U_L(T - T_{amb})]} \Rightarrow F_R\langle\dot{m}\rangle = F'\langle\dot{m}\rangle \frac{L_h\langle\dot{m}\rangle}{L}\left[1 - exp\left(-\frac{L}{L_h\langle\dot{m}\rangle}\right)\right] \tag{20}$$

Here, L_h is a characteristic heating length (Equation 21). The dependence of h_a, *F'*, L_h, and F_R on mass flow rate m is indicated in Equations (19), (20), and (21).

$$L_h\langle\dot{m}\rangle = \frac{\dot{m} C_{p,m}}{F'\langle\dot{m}\rangle P_{ex} U_L} \tag{21}$$

The thermal efficiency of the receiver tube η_r can be expressed as a compact expression using Equations (17) to (21), resulting in Equation (22). T_{amb} may differ slightly from the atmospheric temperature Tatm due to the effective temperatures of the sky and ground.

$$\eta_r = \frac{\dot{Q}_u}{\dot{q}_s P_{ex} L} = F_R\langle\dot{m}\rangle\left[1 - \frac{U_L(T_{in} - T_{amb})}{\dot{q}_s}\right] \tag{22}$$

Combining Equations (18) to (21) determines the mass flow rate (Equation 24), ensuring the desired outlet temperature T_{out}, for a given $\dot{q}_s$ and a non-dimensional slenderness $Sl = L/P_{ex}$. For a given $\dot{q}_s$, L determines the total magnitude of $\dot{Q}_u$, while P_{ex} is determined by D_{ex} (Equation 7). Equation (23) includes the enthalpy difference approximation of Equation (18).

$$T_{out} = \left(\frac{\dot{q}_s C_{p,m}}{U_L}\left[1 - exp\left(-\frac{Sl D_{ex}^2 \pi^2 U_L}{\left(1 + \frac{U_L D_{ex}}{h_a D}\right)\dot{m} C_{p,m}}\right)\right]\left(1 - \frac{U_L(T_{in} - T_{amb})}{\dot{q}_s}\right) + C_{p,in}T_{int}\right) \Big/ C_{p,ou} \tag{23}$$

III.3. Drying kinetics

III.3.1. Moisture content

The process of moisture removal was monitored by regularly weighing the samples until their weight remained constant, indicating the end of moisture loss. Before the start of drying, the initial weights of the samples were accurately measured using a precision balance. The moisture content was subsequently calculated using the following equation:

$$Mc = \frac{M0 - Mf}{M0} \times 100 \tag{24}$$

Here, *Mc* refers to the initial moisture content of the samples on a wet basis (%), M_0 represents the initial mass of the samples before drying, and M_f indicates the final mass of the samples after the drying process.

III.3.2. Mathematical modeling of drying kinetics

To evaluate the drying kinetics, the moisture ratio (MR) of the samples was calculated using the following equation:

$$MR = \frac{Mt - Me}{M0 - Me} \tag{25}$$

In this equation, Mt, Me, and M_0 represent the moisture content (dry basis) at time t, at equilibrium, and at the initial time (t = 0), respectively. The drying kinetics were analyzed using thin-layer drying models. Among ten proposed models (as listed in Table III.1), the most suitable model was selected based on several statistical criteria. The coefficient of determination (R^2) served as a primary metric for identifying the model that best represented the drying behavior. In addition, other statistical indicators such as the reduced chi-square (χ^2) and the root mean square error (RMSE) were employed to evaluate the goodness of fit.

Table III.1. Mathematical Models for Thin-Layer Drying

Model	Expression
Newton	$MR = \exp(-kt)$
Page	$MR = \exp(-kt^{n})$
Henderson and Pabis	$MR = a\exp(-kt)$
Modified Page	$MR = \exp(-(kt)^{n})$
Logarithmic	$MR = a\exp(-kt) + c$
Midilli-Kucuk	$MR = a\exp(-kt^{n}) + bt$
Approximation of Diffusion	$MR = a\exp(-kt) + (1-a)\exp(-kbt)$
Two-Terms	$MR = a\exp(-k1t) + b\exp(-k2t)$
Verma et al	$MR = a\exp(-k1t) + (1-a)\exp(-k2t)$
Two-Terms Exponential	$MR = a\exp(-kt) + (1-a)\exp(-kat)$

These coefficients were determined as follows **[69]**:

$$R^2 = 1 - \frac{\sum_{i=1}^{N}(MR_{exp,i} - MR_{pre,i})^2}{\sum_{i=1}^{N}(\overline{MR_{exp,\iota}} - MR_{pre,i})^2} \tag{26}$$

$$\chi^2 = \frac{\sum_{i=1}^{N}(MR_{exp,i} - MR_{pre,i})^2}{N-n} \tag{27}$$

With

$$\overline{MR_{exp,\iota}} = \frac{\sum_{i=1}^{N} MR_{exp,i}}{N} \tag{28}$$

Where $MR_{exp,i}$ and $MR_{pre,i}$ represent the experimentally measured and model-predicted moisture ratios, respectively. N denotes the total number of observations, and n is the number of constants in the drying model.

III.3.3. Effective diffusivity coefficient

The mass transfer process of moisture content, characterized by the effective diffusivity coefficient (D_{eff}), plays a fundamental role in this study. Moisture diffusion is driven by concentration gradients, and precise estimation of this coefficient is essential for accurately modeling the mass transfer phenomenon according to Fick's law. In this context, the mathematical formulation of Fick's second law is expressed in Equation 29 **[70]**:

$$\frac{\partial MR}{\partial t} = \nabla\left[D_{eff}\nabla MR\right] \tag{29}$$

By assuming a constant value for "D_{eff}," the equation can be simplified and expressed as Equation 13.

$$\frac{\partial MR}{\partial t} = D_{eff} \nabla^2 MR \tag{30}$$

The dried product leaves were modeled as uniform plates subjected to unsteady (non-stationary) drying conditions, with an initially uniform moisture distribution and a constant moisture concentration at the surface. Assuming an infinite, rigid plate with negligible shrinkage or swelling, uniform initial moisture content, negligible external mass transfer resistance, and constant effective diffusivity, the analytical solution to Fick's second law, as developed by Crank **[71]**, is represented by Equation 31:

$$MR = \frac{8}{\pi^2} \sum_{n=0}^{\infty} \frac{1}{(2n+1)^2} exp \left(\frac{-(2n+1)^2 \pi^2 D_{eff} t}{4r^2}\right) \tag{31}$$

For extended drying times, the higher-order terms in the series (where n ≥ 1) become negligible in comparison to the first term. As a result, the equation simplifies to Equation 32.

$$MR = \frac{8}{\pi^2} exp \left(\frac{-\pi^2 D_{eff} t}{4r^2}\right) \tag{32}$$

Rearranging Equation 32 yields:

$$Ln(MR) = Ln\left(\frac{8}{\pi^2}\right) - \left(\frac{\pi^2 D_{eff}}{4r^2}\right) t \tag{33}$$

The experimental drying data are expressed as the natural logarithm of the moisture ratio, *ln(MR)*, plotted against drying time at various temperatures. The effective diffusivity coefficient can be determined using the slope of the resulting linear relationship, as described by Equation 30:

$$Slope(k) = \left(\frac{-\pi^2 D_{eff}}{4r^2}\right) \tag{34}$$

Finally, the effective diffusivity coefficient (D_{eff}) can be calculated using Equation 35:

$$D_{eff} = \frac{Slope\ (k)}{-\pi^2}\ 4r^2 \tag{35}$$

In this context, ($\boldsymbol{D_{eff}}$) represents the effective diffusivity measured in (m²/s), while (***t***) denotes time (s), (***r***) refers to the half-thickness of the material sample (m), and (***n***) is a positive integer indicating the order of the diffusion process. By applying the slope method in conjunction with the aforementioned equations, the effective diffusivity coefficient ($\boldsymbol{D_{eff}}$) can be accurately determined, providing deeper insight into the mechanisms of moisture transfer during drying. This coefficient plays a crucial role in analyzing and optimizing drying kinetics, as well as enhancing the design and performance of drying systems.

III.4. Economic analysis

Economic evaluation is a key factor in assessing the potential public acceptance and viability of a project. In the context of a solar dryer project, a thorough economic analysis encompasses three fundamental aspects: annual cost, lifecycle savings, and payback period. These components collectively provide a clear understanding of the project's financial feasibility and long-term benefits.

III.4.1. Annualized cost

The annualized cost accounts for several key factors, including the annualized salvage value (Sa), the cost of electrical energy (C_{el}), maintenance expenses (C_m), and the cost of the dryer's components (C_{ac}). The total annual cost is calculated using the following expression **[72, 73]**:

$$AC = C_{el} + C_{ac} + C_m - S_a \quad (36)$$

Where S_a and C_{ac} are determined using the following formulas:

$$S_a = S \times \frac{i}{(1+i)^n - 1} \quad (37)$$

$$C_{ac} = C_{cd} \times \frac{i(1+i)^n}{(1+i)^n - 1} \quad (38)$$

Here, C_{cd} denotes the capital cost of the solar dryer, which is 521 USD, and S represents the salvage value, calculated as 10% of C_{cd}.

The annual cost of electrical energy (C_{el}) needed to operate the dryer is calculated based on the energy consumed by the fan, using Algeria's electricity unit price (C_{ee}) of 4.1 DZD, equivalent to approximately 0.030 USD.

$$C_{el} = C_{ee} \times W_p \times t \quad (39)$$

The cost required to dry one kilogram of the product (CD_{kg}) is calculated by dividing the total annualized cost by the annual quantity of dried product (M_{year}), as follows:

$$CD_{kg} = \frac{AC}{M_{year}} \quad (40)$$

III.4.2. Life cycle savings

The savings per drying day are calculated as the difference between the cost of the primary raw material intended for drying and the cost per kilogram of the final dried product obtained from the dryer:

$$C_{dry} = C_{fre} \times \frac{M_{fre}}{M_{dry}} \quad (41)$$

For the solar dryer, the cost per kilogram of dried product (C_{drys}) is calculated by summing the initial cost of the fresh item before drying (C_{dry}) and the drying cost per kilogram (CD_{kg}), as expressed in the following equation:

$$C_{drys} = C_{dry} + CD_{kg} \tag{42}$$

The savings per kilogram of dried product obtained (B_{kg}), savings per batch (B_b), and savings per drying day (B_d) in the reference year are calculated using the following formulas:

$$B_{kg} = C_{bdp} - C_{drys} \tag{43}$$

$$B_b = B_{kg} \times M_{dry} \tag{44}$$

$$B_d = \frac{B_b}{D_b} \tag{45}$$

The total annual savings of the drying system over its entire operational lifespan (B_j) is calculated as follows:

$$B_j = B_d \times D_{year} \times (1 + r)^{j-1} \tag{46}$$

III.4.3. Payback period

The payback period refers to the length of time needed to recover the initial investment made in the drying system. Furthermore, as noted by:

$$P_p = \frac{\ln(1 - \frac{C_{cd}}{B_1}(i - r))}{\ln(\frac{1+r}{1+i})} \tag{47}$$

III.5. Conclusion

In conclusion, this chapter focused on developing and validating numerical models to simulate solar drying systems, using both mathematical and physical approaches, in preparation for their comparison with experimental data. This methodology contributed to a deeper understanding of how different configurations affect system performance, with the results to be used in the next chapter for analyzing and evaluating the practical effectiveness of solar drying technologies.

The chapter also addressed drying kinetics through the study of moisture content evolution, mathematical modeling of the drying behavior, and the calculation of the effective moisture diffusivity. On the economic side, the mathematical foundations for evaluating the solar dryer’s feasibility were presented, focusing on three key metrics: annual cost, life-cycle savings, and payback period. These elements provide a basis for assessing financial viability and promoting the broader adoption of the system.

Chapter IV

Experimental Study and Methods

Chapter IV:
Experimental Study and Methods

IV.1. Introduction

In this chapter, we present the experimental study conducted in a sunny outdoor environment near the Mechanical Engineering Laboratory at El-Oued University, in collaboration with the Renewable Energy Development Unit in Arid Zones (UDERZA). This chapter provides a comprehensive overview of the meteorological and climatic conditions of the study area, assesses the solar energy potential, and explores the environmental interactions between the oasis and desert surroundings of El Oued. The experimental work focuses on evaluating and improving the performance of the innovative solar dryer through four main objectives: assessing its operation under real and typical conditions, examining the impact of integrating Phase Change Materials (PCM) on thermal performance, testing the enhanced system's ability to handle fluctuating weather conditions, and performing a comparative analysis of the drying process under different scenarios including using the original solar dryer, the PCM-enhanced version, shaded environments, and direct sunlight. The methodology involves measuring key parameters such as temperature, solar radiation intensity, wind speed, and airflow velocity, along with monitoring drying rates and moisture content. These measurements enable a thorough evaluation of dryer performance under both stable and variable climatic conditions.

IV.2. Meteorological and climate characteristics of the study area

The meteorological and climate characteristics of the study area are essential for evaluating the solar dryer's performance under real conditions. Factors such as solar radiation, temperature, wind, and humidity directly influence drying efficiency. They also help interpret the results and assess the system's applicability in similar climatic regions.

IV.2.1 The potential of solar energy in the experimental area

The experiments were conducted using the fabricated solar dryer in the open field of the Mechanical Engineering Laboratory at El Oued University, Algeria. It is important to highlight that approximately 77% of Algeria's territory is classified as arid or semi-arid. El Oued is one such region, situated in an oasis zone in the northern part of the Sahara. According to the Köppen-Geiger climate classification, it falls under the BWh category, which denotes a hot desert climate. The region is characterized by the following features:

Table IV.1. The characteristics and meteorological data of the region El Oued [**58, 74**, **75, 76]**

The characteristics and meteorological data	***Valuer***
Located west of the Mediterranean Sea on the Tunisian coast	361.7 km
Latitude	33°23’47” N
Longitude	6°51’43” E
The altitude above the sea level	69 m
Rate of sunny days per year	78%
The annual daily average of global solar irradiance at horizontal surfaces	6.25 kWh/m^2
The annual duration of Daylight	3328.17 hours
The annual average temperature change can reach	30.23° C
The annual average Air temperature	21.5° C
The annual average rainfall distribution	66.91 mm
The annual average relative humidity	48.7 %

The geographical location of El-Oued province is highlighted in red on the map, which presents solar resource data obtained from the Global Solar Atlas (GSA) **[77]**. The map illustrates global horizontal irradiation levels, as shown in Figure IV.1.

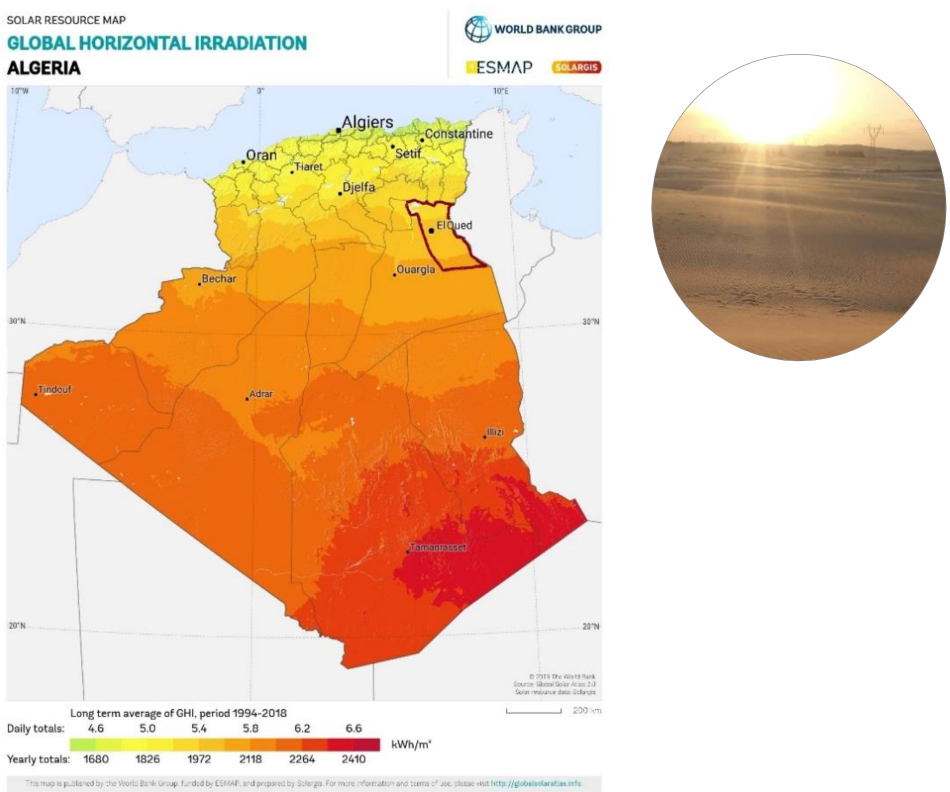

Fig. IV.1. Solar resource map showing global horizontal irradiation and the geographical location of El Oued province, based on data from the Global Solar Atlas (GSA) **[77].**

The city benefits from excellent solar potential year-round, primarily due to its favorable geographical location. The average daily solar radiation received on a horizontal surface is approximately 6250 Wh/m², as illustrated in Figures IV.1 and IV.2.

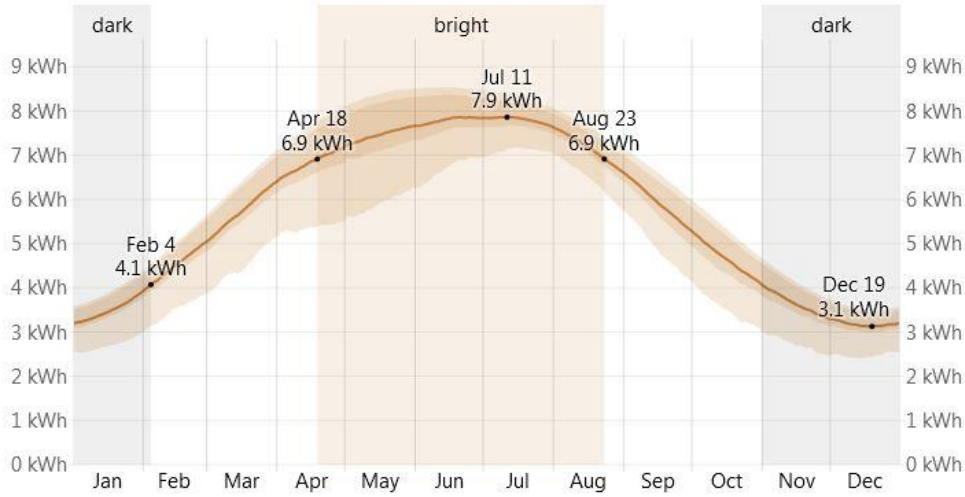

Fig. IV.2. Average Daily Shortwave Solar Radiation Received in El Oued **[74].**

Based on the sun path diagrams for El Oued (Figure IV.3), the solar altitude and azimuth angles can be directly determined for any day of the year and at any hour. These diagrams clearly illustrate the variation between the solar angles during the summer and winter solstices, as well as the time interval between them.

Given this divergence, and to ensure optimal solar capture throughout the year, it is proposed that the solar dryer be equipped with a dual-axis solar tracking system. This recommendation stems from the performance limitations of single-axis trackers, which are less effective in covering the full seasonal range of solar angles.

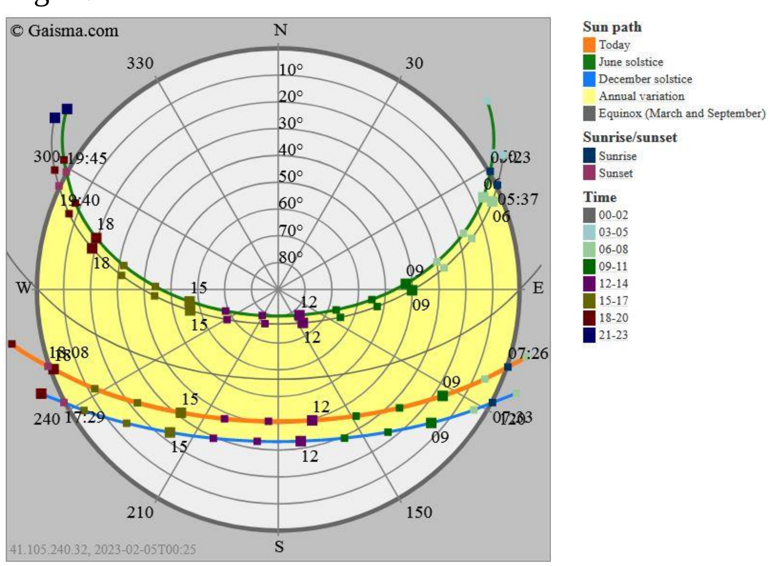

Fig. IV. 3. Sun Path Diagrams for El Oued, sourced from *Gaisma.com* **[78].**

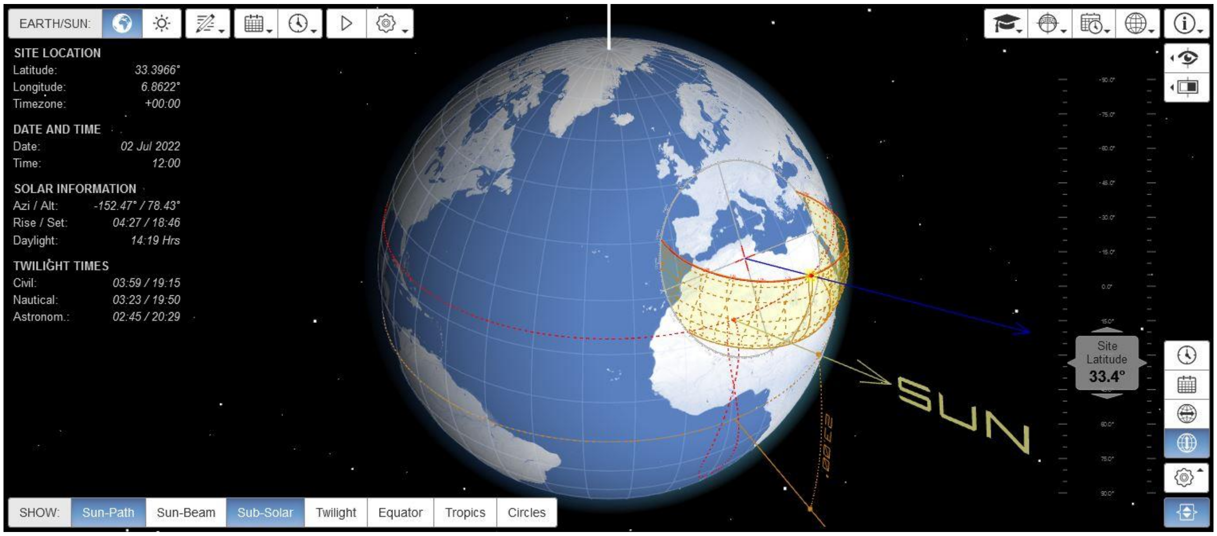

Fig. IV.4. DP Earth/Sun for El Oued, from *drajmarsh.bitbucket.io* **[79].**

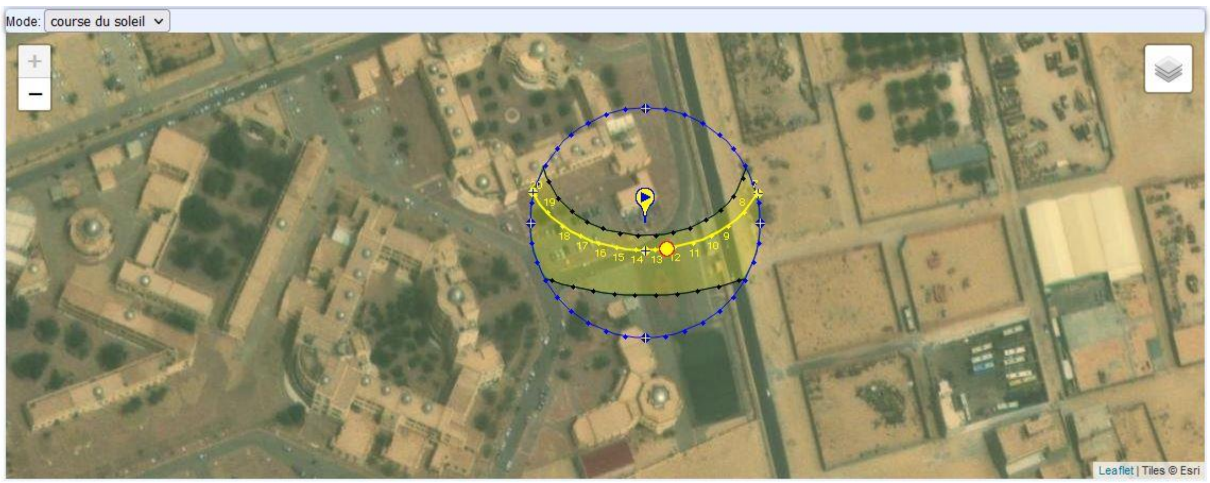

Fig. IV.5. Local position of Sun path at El Oued University's study area, from *SunEarthTools.com* **[80].**

IV.3. Experimental setup and methodology

IV.3.1. Experiment 1: The solar dryer (SDPTC) under real and typical operating conditions.

The study methodology relies on experimental work under clear sky conditions and stable weather in the previously designated sunny experimental field. Various parameters, including solar radiation, wind speed, and temperature, were measured using different instruments such as a Pyranometer, Temperature Recorder, Thermocouples, and Anemometer. Data were collected hourly from 6:00 a.m. to 6:00 p.m, during the first week of July.

Solar tracking was performed every 15 minutes using a semi-automatic system to maximize solar energy capture. This setup is illustrated schematically and through photographs, as shown in Figures IV.8 and IV.9.

(a) Local Time at 11: 00 (b) at 13: 00 (c) at 15: 00 (d) at 17: 00

Fig. IV.8. Various positions of the solar dryer equipped with a PTC system, tracking the sun along two axes throughout the day.

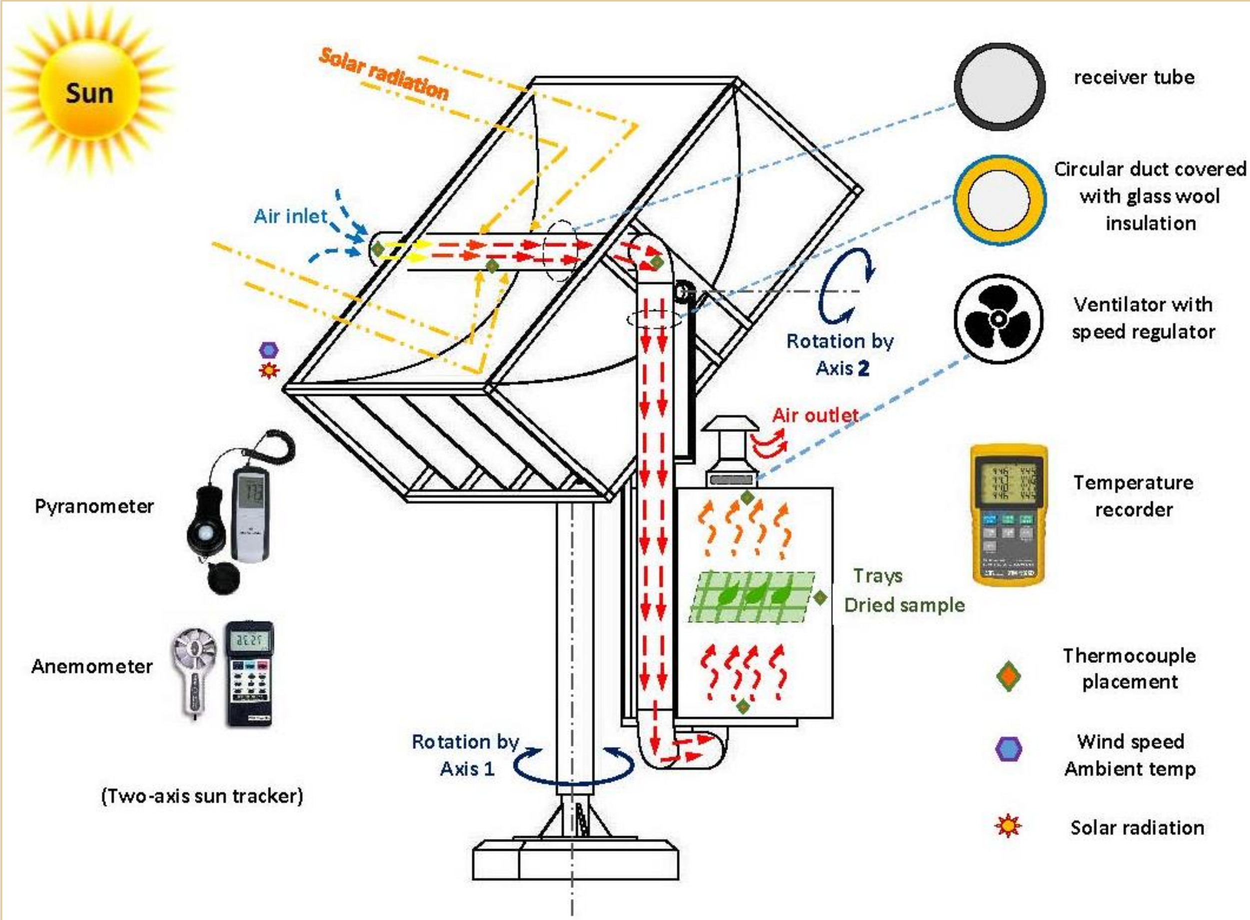

Fig. IV. 9. Schematic representation of the experimental setup of the solar dryer assisted by (PTC)

This experiment aims to utilize solar energy to produce hot air through a parabolic trough concentrator (PTC) that is mounted on a two-axis tracker to efficiently collect sunlight. The receiver tube, situated along the focal line of the PTC, efficiently absorbs sunlight and converts it into thermal energy. The wall of the receiver tube acts as the site of thermal conversion, where concentrated solar radiation is converted into high-temperature heat, which is then used to heat the air required for the drying process. The tracking of the sun was carried out by monitoring the solar radiation incident on the parabolic trough concentrator, using a Pyranometer (model: PYR-1307) placed in an open, unshaded location adjacent to the solar dryer. Wind speed was recorded using an Anemometer (model: AM-4206). Temperature measurements at various points within the solar dryer were taken using K-type thermocouples. These included the inlet and outlet of the receiver tube, the tube wall, the inlet and outlet of the drying chamber, as well as the ambient temperature. To ensure continuous data monitoring, a data Acquisition system (model: BTM-4208SD) was connected to the outputs of the Pyranometer and the Thermocouples. The experimental setup is provided in Figures IV.8 and IV.9.

IV.6. Economic study

IV.6.1. The cost of the setup's materials for the prototype solar dryer

To provide a low-cost solar dryer, an experimental system was built using materials selected for their malleability, affordability, and availability in the local market. Table IV.4 provides a detailed breakdown of the costs associated with the various materials and components required for constructing the solar dryer. The total cost of the entire setup amounts to 76,350 DZD, which is approximately USD 520, based on the exchange rate of 1 USD = 146.40 DZD.

Table IV.4. Material cost for construction **[58].**

Equipment/material used	Quantity	Total Price in DZD
metal structure (flat bar, angle, square Rect tubing, H beam, Steel Pipes …)	--	20000
tapered roller bearing	2	1800
Concrete foundation (Sand, gravel, Cement, rebar)	--	4000
receiver tube (galvanized steel)	2.2 m	3500
matte black paint	(2 kg)	800
Reflector (ordinary mirror)	3 m^2	6000
drying chamber (sandwich panels with polyethylene foam insulation)	1	5000
Ventilator	1	1200
Tracker motor (actuator Parabola)	1	4500
Chimney	1	400
Glue, transparent silicone	3	1050
insulating adhesive tape	3	900
PVC suction hose (80 mm)	2 m	1600
glass wool insulation	2 m^2	600
Cost of welding	--	10000
Cost of Lathing	--	5000
Cost of glass agent	--	5000
Transportation and installation cost	--	5000
Totale cost (146.40 DZD=1$)		**76350 DZD ≈ 521 US Dollar**

Chapter V

Results and discussions

Chapter V:
Results and Discussions

V.1. Introduction

This chapter presents the results and discussions related to the experimental work conducted in this thesis. The performance of the innovative solar dryer was evaluated and analyzed through a series of field experiments carried out in a real desert environment. The assessment focused on four main aspects: first, evaluating the dryer's performance under actual operating conditions and validating the model by comparing experimental data with numerical simulations; second, analyzing the impact of integrating Phase Change Materials (PCM) on the system's thermal efficiency; third, assessing the system's ability to maintain effective operation under fluctuating weather conditions; and fourth, performing a comparative analysis of drying effectiveness under various scenarios (with PCM, without PCM, in the shade, and under direct sunlight).

In addition, this chapter includes an economic analysis that highlights the system's financial feasibility, confirming its technical efficiency and cost-effectiveness for agricultural solar drying applications. These findings support the system's potential as a sustainable solution in regions with high solar radiation.

V.2. Experiment 1: The solar dryer (SDPTC) under real and typical operating conditions.

V.2.1. Meteorological conditions during the experimental day: Real-time solar irradiance and ambient temperature

To ensure the reliability and repeatability of the solar drying experiment, real-time meteorological data were recorded throughout the test, from 6:00 AM to 6:00 PM. As illustrated in Figure V.1, hourly variations in solar irradiance and ambient temperature were observed under clear sky conditions. The maximum solar irradiance reached 1012 W/m² at solar noon, with an average value of approximately 750 W/m². Similarly, ambient temperature peaked at 45.1 °C, while the average temperature during the daylight period was 40.8 °C. These meteorological conditions provided a favorable environment for evaluating the thermal and drying performance of the system under realistic operational scenarios.

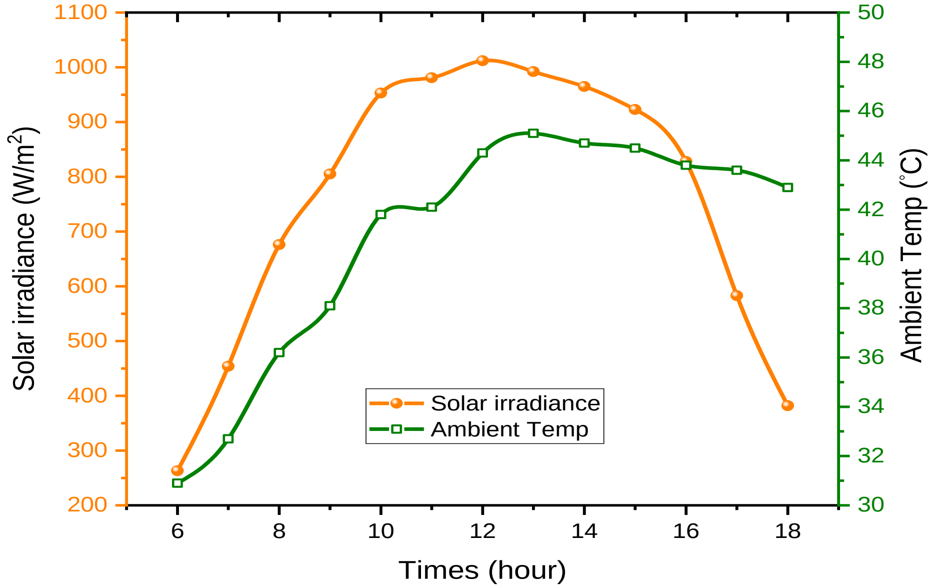

Fig. V.1. Real-time solar irradiance and ambient temperature measurements

V.2.2. Thermal performance of the solar dryer

V.2.2.1. Thermal behavior of the receiver

To evaluate the effectiveness of the solar dryer in converting solar radiation into usable thermal energy, the receiver wall temperatures were monitored in real-time alongside the solar irradiance throughout the experiment. The results revealed a clear proportional relationship between the incident solar radiation and the receiver wall temperature, reflecting the system's thermal response under actual operating conditions.

Figure V.2 illustrates the variation in solar irradiance and receiver wall temperature, highlighting this thermal correlation. As solar radiation increased, the receiver wall temperature rose progressively over time, with peak values recorded at 13:00, 992 W/m² for solar irradiance, and 115 °C for receiver temperature, as shown in Figures V.2 and V.3.

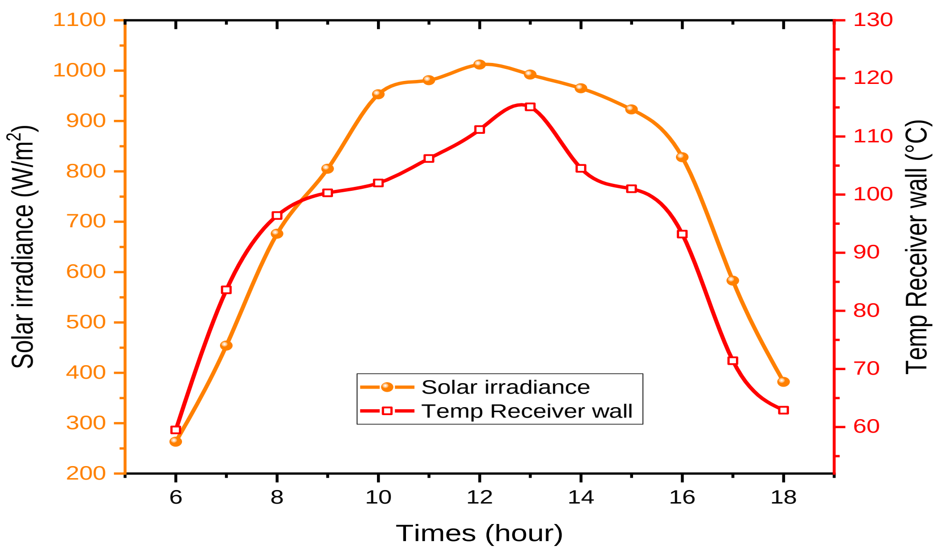

Fig. V.2. Evolution of solar radiation and receiver wall temperature T5

Despite occasional weather fluctuations, such as short wind gusts reaching 2.96 m/s during certain periods, the experiment demonstrated that hot air could be efficiently generated inside the receiver tube for the drying process, even in the absence of a glass cover. The influence of wind speed on the surface heat loss of the receiver wall was also observed, emphasizing the importance of proper thermal insulation and design optimization to counteract variable environmental conditions.

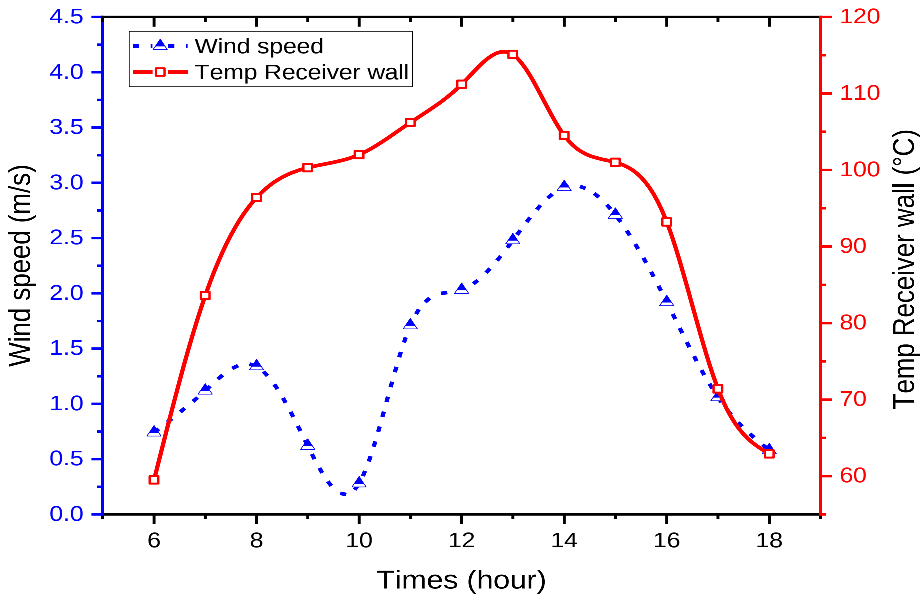

Fig. V.3. Effect of wind speed on the heat of the receiver wall

Figures V.4 and 5 illustrate the temporal trends of both solar irradiance and the temperature difference (ΔT) between the inlet and outlet air in the receiver tube. As shown in the results, the temperature difference (ΔT) increases significantly with the rise in solar irradiance and ambient temperature, indicating improved heat transfer efficiency within the receiver tube. This difference reaches its peak at midday, when ambient weather conditions are more stable, allowing the system to achieve a more consistent thermal performance. However, some temporary fluctuations in ΔT were observed due to wind variations, which affect heat loss from the receiver surface. The relationship between ΔT and solar radiation serves as a direct indicator of the system's ability to convert solar energy into effective heat used for air heating in the drying process.

This performance highlights the system's good thermal efficiency, as the temperature difference reflects the receiver's capacity to absorb solar energy and raise the temperature of the flowing air. The more stable and elevated this difference is, the more it demonstrates the effectiveness of the receiver's thermal design in minimizing heat losses under variable weather conditions.

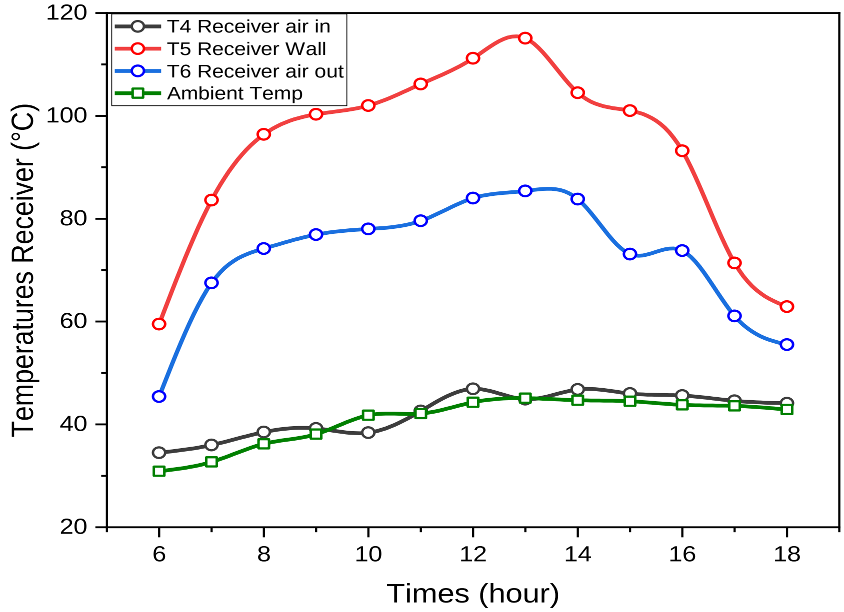

Fig. V.4. Evolution of receiver temperatures T_4, T_5, T_6, T_{amb}

.

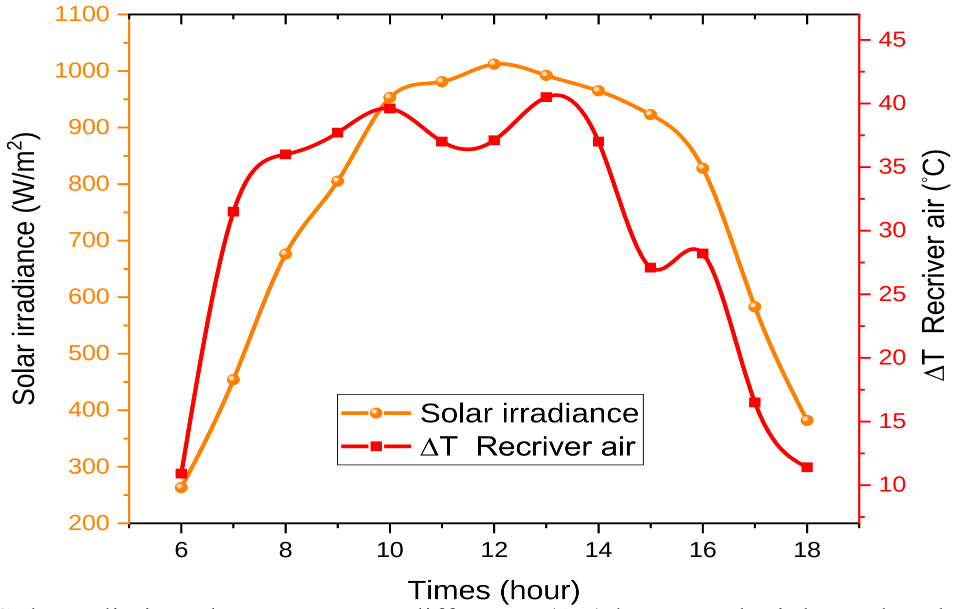

Fig. V.5. Solar radiation, the temperature difference (ΔT) between the inlet and outlet of the receiver air

The thermal efficiency of the system (ηth) was calculated by comparing the thermal energy gained by the air with the incident solar energy on the collector. As shown in Figure V.6, the thermal efficiency exhibits a fluctuating trend throughout the day, influenced by various climatic factors such as solar irradiance, wind speed, and the temperature difference (ΔT) between the inlet and outlet air of the receiver.

During certain periods, the system achieves higher performance, with a peak thermal efficiency of 45.25%. However, in other intervals, the efficiency drops below 20%, mainly due to sudden variations in weather conditions. Notably, the system demonstrates more stable performance around noon, when solar radiation is at its peak, with an average daily thermal efficiency recorded at 25.93%.

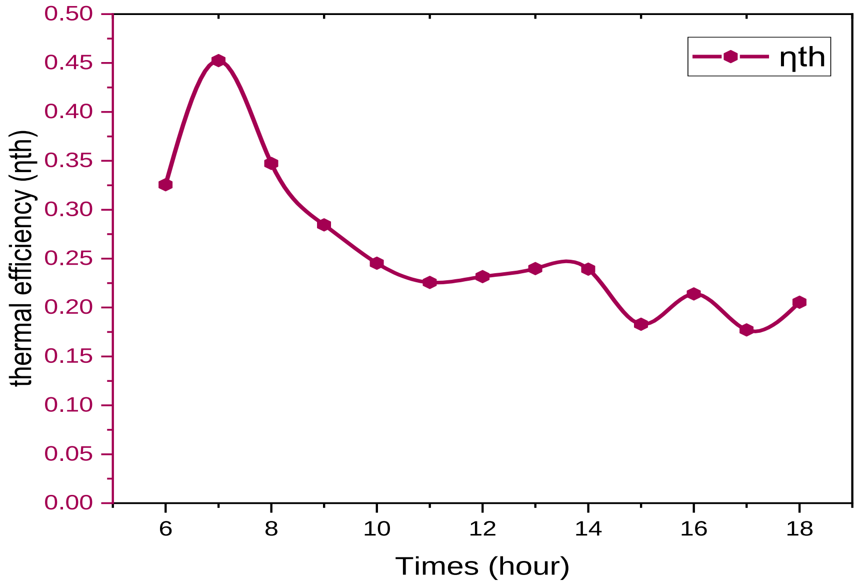

Fig. V.6. Thermal efficiency (ηth)

V.2.2.2. Thermal Behavior within the Drying Chamber

Figure V.7 illustrates the temporal variation of ambient temperature alongside the temperatures measured inside the drying chamber, revealing a strong correlation between the two. As ambient temperature increases throughout the day, the internal chamber temperature also rises progressively, reaching a peak of 68 °C at around 13:00. This behavior highlights the system's responsiveness to external thermal conditions.

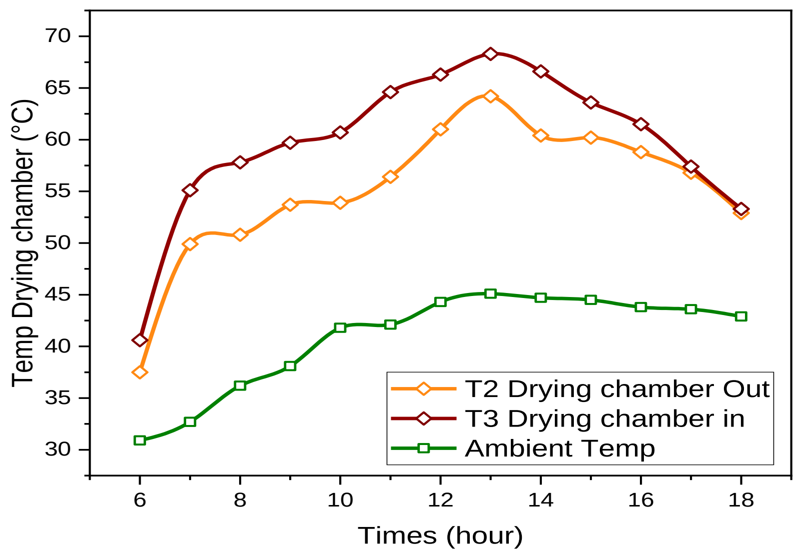

Fig. V.7. Temporal variation of ambient and drying air temperatures during the drying test

The data also demonstrate the dynamic nature of the temperature difference (ΔT) between the ambient air and the drying air. At sunrise and sunset, ΔT is relatively modest around 10 °C due to the mild environmental conditions. As solar radiation intensifies with the rising sun, the heating process within the drying system initiates, resulting in a steady increase in ΔT.

At midday (13:00), this temperature difference reaches a maximum value of 33 °C, corresponding to the peak solar radiation and maximum thermal absorption by the solar dryer. The cylindrical-parabolic solar collector plays a crucial role in this performance, effectively capturing and concentrating solar energy to significantly increase drying air temperature.

Overall, the observed temperature trends confirm the system's ability to efficiently generate and maintain hot air within the drying chamber. The substantial ΔT at peak hours is a clear indicator of the dryer's capacity to support the effective dehydration of agricultural products. These insights are essential for assessing system performance and guiding operational strategies for different drying scenarios.

V.2.3. Thermal model calibration and validation through experimental and simulated data comparison

V.2.3.1. Model validation

In the process of validating our model, we scrutinized the simulated and experimental outlet air temperatures of the receiver, as illustrated in Fig. 17. The critical parameter in this validation process was the heat transfer coefficient (*UL*), which governs the local heat losses from the external wall of the receiver tube, characterized by a temperature (T_w), towards the ambient environment at a temperature (T_{amb}). To enhance the model's accuracy, *UL* was meticulously calibrated to achieve optimal alignment with the experimental data.

Remarkably, our model exhibits a commendable agreement with the experimental observations, particularly during daylight hours. The simulated outlet air temperature of the receiver was rigorously validated against experimental data obtained from a state-of-the-art solar dryer. This solar dryer is equipped with a parabolic trough concentrator (PTC) and features a dual-axis solar tracker. The experiments were conducted in the open field of the Mechanical Engineering Laboratory situated at El Oued University in Algeria. The validation process solidifies the reliability and predictive capability of our model, showcasing its robust performance in simulating the intricate dynamics of the solar drying system under investigation.

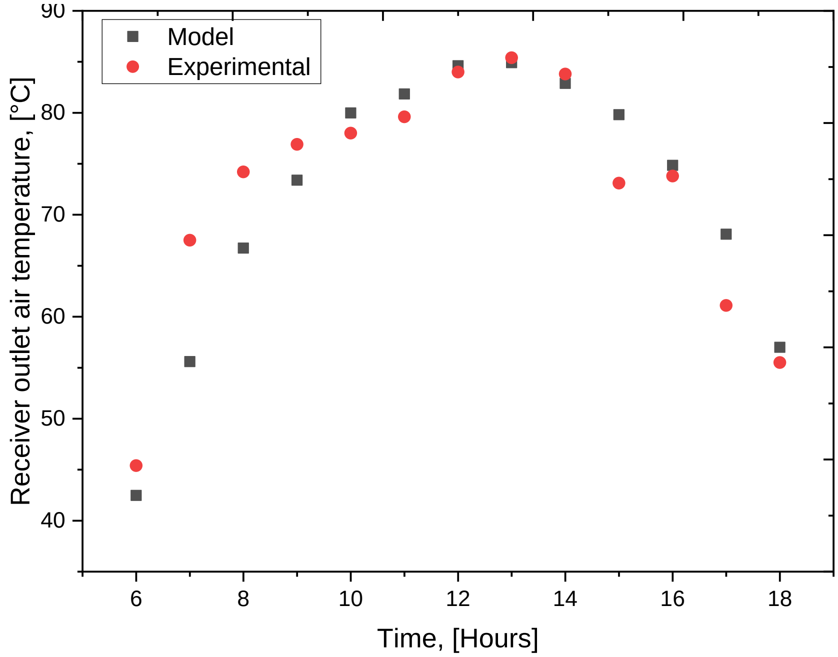

Fig. V.8. Comparison between simulated and experimental outlet temperature

V.2.3.2. Effect of basic parameters on the outlet air temperature of the receiver

In this section, we delve into an exploration of the pivotal parameters influencing the outlet air temperature of the receiver within the innovative solar dryer, augmented by a parabolic trough concentrator (PTC) featuring a dual-axis solar tracker. Our investigation is conducted on a clear sky day, precisely on July 2nd, 2022, at El Oued University in the southeastern region of Algeria. Comprehensive details outlining the specifications of the PTC employed in our simulations are provided in Tables II.1, 2, 3, and 4.

V.2.3.2.1. Air mass flow rate influence:

Examining Figure V.9 reveals the variation in the outlet air temperature of the receiver at distinct times of the day. Notably, a discernible trend emerges the outlet air temperature experiences a decline with an escalation in the air mass flow rate. This observation holds for distinct time points during the day, specifically at 10:00 AM, 12:00 PM, and 5:00 PM.

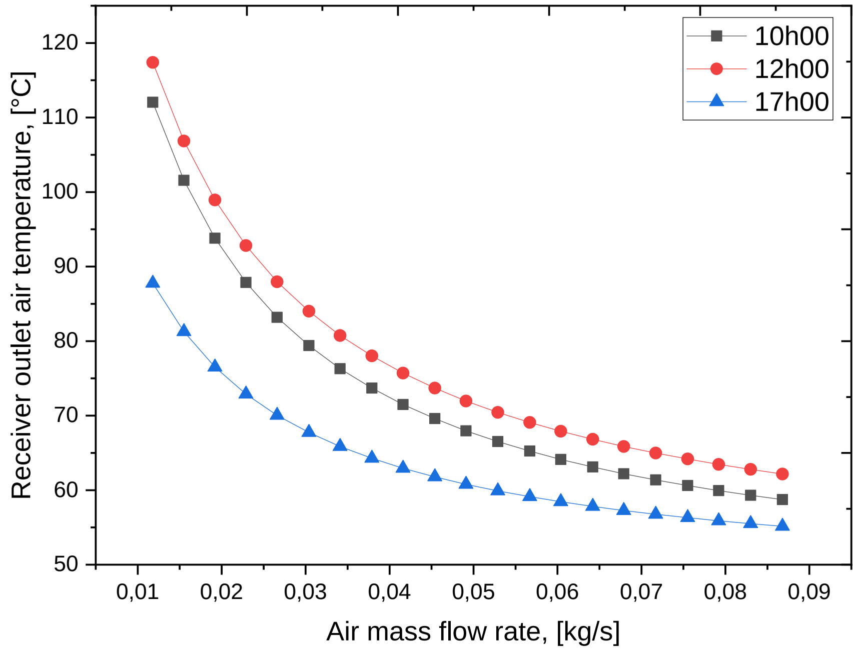

Fig. V.9 Receiver outlet air temperature variations with mass flow rate at different time

V.2.3.2.2. Receiver tube diameter impact:

Figure V.10 presents an in-depth exploration of how the outlet air temperature of the receiver evolves. Intriguingly, a consistent pattern is discerned as the diameter of the galvanized steel receiver tube, devoid of a glass cover, increases, and there is a corresponding decrease in the outlet air temperature. This trend is evident across multiple time intervals during the day, spanning from 10:00 AM to 6:00 PM.

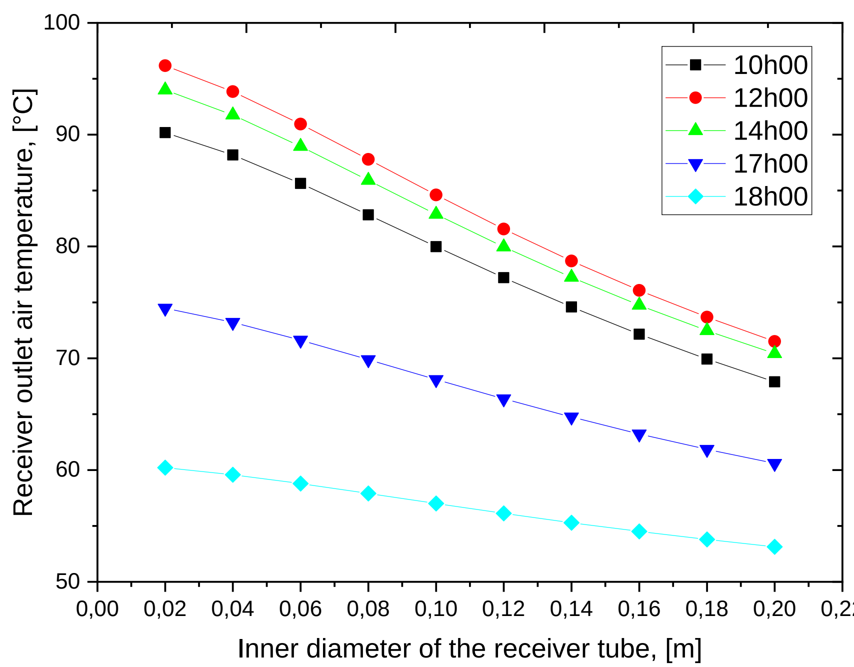

Fig. V.10 Receiver outlet air temperature variations with receiver tube diameter at different time

These findings illuminate the intricate interplay between key parameters and the outlet air temperature of the receiver, contributing valuable insights into the performance dynamics of the solar drying system under investigation.

General Conclusion

General Conclusion

This thesis set out to tackle a common and persistent problem in solar drying systems: their poor performance during late afternoon hours and under changing weather conditions. These shortcomings are mainly due to the lack of solar tracking and reliable thermal energy storage, which limits the system's ability to make full use of available solar radiation throughout the day.

To address this, a new solar dryer was designed, built, and tested. The system brings together three essential innovations: a parabolic trough collector (PTC) that concentrates solar energy, a dual-axis tracking system to follow the sun's path and increase energy capture, and a thermal storage unit using phase change materials (PCMs) to retain heat and extend drying beyond daylight hours. The prototype was installed and evaluated under real operating conditions at the University of El Oued, located in the Saharan region of Algeria. A combination of experimental trials, simulations, and economic analyses were carried out to assess its performance.

The work presented here shows that combining solar concentration, tracking systems, and latent heat storage can result in a highly efficient and scalable solar dryer. The system offers a practical solution for reducing post-harvest losses, especially in sun-rich but infrastructure-limited areas like southern Algeria. It also supports broader goals of promoting renewable energy use in agriculture and improving food preservation.

Looking ahead, there are several ways this work could be extended. Future studies might explore PCMs with better thermal properties, test the system on different crops or in other regions, incorporate smart control systems to adjust temperature and airflow automatically, and examine long-term performance across various seasons.

In the final word, this thesis presents an original scientific and technical contribution to the field of solar drying by proposing an efficient, low-cost, and environmentally friendly solution. The outcomes pave the way for practical applications that align with Algeria's goals in food security and energy transition.

References

References

[1] Ministry of Energy, mines and renewable energies. Potentiel Solaire. Available online : https://www.energy.gov.dz/?rubrique=energies-nouvelles-renouvelables-et-maitrise-de-lrenergie&utm (accessed on Mai 2025)

[2] Zahraoui, Y., Khan, M. R. B., AlHamrouni, I., Mekhilef, S., & Ahmed, M. (2021). Status, scenario, and prospective of renewable energy in Algeria: a review. *Energies*, *14*(9), 2354. https://doi.org/10.3390/en14092354.

[3] National Agency for the Promotion and Rationalisation of Energy Use (APRUE) . Available online: https://www.aprue.org.dz/ (accessed on Mai 2025)

[4] International Energy Forum (IEF). Available online: https://www.ief.org/news/algeria-powers-ahead-with-huge-renewable-energy-plans (accessed on Mai 2025)

[5] Tria, D., Alghorbany, A., Muhamad, A. I. B., & Alam, M. M. (2020). Government policies, financial scopes and technological usages for agricultural development and post-harvest loss reduction in Algeria. International Journal of Postharvest Technology and Innovation, 7(4), 335-352. https://doi.org/10.1504/IJPTI.2020.110888

[6] Enerdata. Available online: https://www.enerdata.net/publications/daily-energy-news/algeria-targets-16-gw-renewable-capacity-2035.html (accessed on Mai 2025).

[7] Sabarez, H. T. (2015). Modeling of drying processes for food materials. In modeling food processing operations (pp. 95-127). Woodhead Publishing. https://doi.org/10.1016/B978-1-78242-284-6.00004-0

[8] Kherrafi, M. A., Benseddik, A., Saim, R., Bouregueba, A., Badji, A., Nettari, C., & Hasrane, I. (2024). Advancements in solar drying technologies: Design variations, hybrid systems, storage materials and numerical analysis: A review. Solar Energy, 270, 112383. https://doi.org/10.1016/j.solener.2024.112383.

[9] Shekata, G. D., Tibba, G. S., & Baheta, A. T. (2024). Recent advancements in indirect solar dryer performance and the associated thermal energy storage. Results in Engineering, 24, 102877. https://doi.org/10.1016/j.rineng.2024.102877

[10] Suresh, B. V., Shireesha, Y., Kishore, T. S., Dwivedi, G., Haghighi, A. T., & Patro, E. R. (2023). Natural energy materials and storage systems for solar dryers: State of the art. Solar Energy Materials and Solar Cells, 255, 112276, https://doi.org/ 10.1016/j.solmat.2023.112276.

[11] Lingayat, A., Balijepalli, R., & Chandramohan, V. P. (2021). Applications of solar energy based drying technologies in various industries–A review. Solar energy, 229, 52-68. https://doi.org/10.1016/j.solener.2021.05.058.

[12] Lingayat, A. B., Chandramohan, V. P., Raju, V. R. K., & Meda, V. (2020). A review on indirect type solar dryers for agricultural crops–Dryer setup, its performance, energy storage and important highlights. Applied energy, 258, 114005., https://doi.org/10.1016/j.apenergy.2019.114005.

[13] Kumar, M., Sansaniwal, S. K., & Khatak, P. (2016). Progress in solar dryers for drying various commodities. Renewable and Sustainable Energy Reviews, 55, 346-360, https://doi.org/10.1016/j.rser.2015.10.158.

[14] Phadke, P. C., Walke, P. V., & Kriplani, V. M. (2015). A review on indirect solar dryers. ARPN Journal of Engineering and Applied Sciences, 10(8), 3360-3371.

[15] Metwally, K. A., Oraiath, A. A. T., Elzein, I. M., El-Messery, T. M., Nyambe, C., Mahmoud, M. M., ... & Elwakeel, A. E. (2024). The mathematical modeling, diffusivity, energy, and enviro-economic analysis (MD3E) of an automatic solar dryer for drying date fruits. Sustainability, 16(8), 3506, https://doi.org/10.3390/su16083506.

[16] Srinivasan, G., & Muthukumar, P. (2021). A review on solar greenhouse dryer: Design, thermal modelling, energy, economic and environmental aspects. Solar Energy, 229, 3-21, https://doi.org/10.1016/j.solener.2021.04.058.

[17] Faraj, K., Khaled, M., Faraj, J., Hachem, F., & Castelain, C. (2021). A review on phase change materials for thermal energy storage in buildings: Heating and hybrid applications. Journal of Energy Storage, 33, 101913. https://doi.org/10.1016/j.est.2020.101913.

[18] Fang, X., Fan, L. W., Ding, Q., Yao, X. L., Wu, Y. Y., Hou, J. F., ... & Hu, Y. C. (2014). Thermal energy storage performance of paraffin-based composite phase change materials filled with hexagonal boron nitride nanosheets. Energy conversion and management, 80, 103-109. https://doi.org/10.1016/j.enconman.2014.01.016.

[19] Agrawal, A., & Sarviya, R. M. (2016). A review of research and development work on solar dryers with heat storage. International Journal of Sustainable Energy, 35(6), 583-605. https://doi.org/10.1080/14786451.2014.930464.

[20] Monicka, A. A., Shree, P., Freeda Blessie, R., Tazeen, H., Navaneetham, B., Sheryl Andria, S., & Brusly Solomon, A. (2024). A comprehensive review of indirect solar drying techniques integrated with thermal storage materials and exergy-environmental analysis. Environment, Development and Sustainability, 1-45. https://doi.org/10.1007/s10668-024- 04755-7, 0123456789.

[21] Ndukwu, M. C., Ibeh, M., Okon, B. B., Akpan, G., Kalu, C. A., Ekop, I., ... & Bennamoun, L. (2023). Progressive review of solar drying studies of agricultural products with exergoeconomics and econo-market participation aspect. Cleaner Environmental Systems, 9, 100120. https://doi.org/10.1016/j. cesys.2023.100120.

[22] Du, K., Calautit, J., Wang, Z., Wu, Y., & Liu, H. (2018). A review of the applications of phase change materials in cooling, heating and power generation in different temperature ranges. Applied energy, 220, 242-273. https://doi.org/10.1016/j.apenergy.2018.03.005.

[23] Tyagi, V. V., & Buddhi, D. P. C. M. (2007). PCM thermal storage in buildings: A state of art. Renewable and sustainable energy reviews, 11(6), 1146-1166, https://doi.org/10.1016/j.rser.2005.10.002.

[24] Aghamohammadi, A., & Foulaadvand, M. E. (2023). Efficiency comparison between tracking and optimally fixed flat solar collectors. Scientific Reports, 13(1), 12712.

[25] Kamarulzaman, A., Hasanuzzaman, M., & Rahim, N. A. (2021). Global advancement of solar drying technologies and its future prospects: A review. Solar Energy, 221, 559-582 . https://doi.org/10.1016/j.solener.2021.04.056.

[26] Nagarajan S, Barshilia H, Rajam K. (2010). Review of sputter deposited mid- to high-temperature solar selective coatings for Flat Plate/Evacuated tube collectors and solar thermal power generation applications.

[27] Bellos, E., & Tzivanidis, C. (2019). A review of concentrating solar thermal collectors with and without nanofluids. Journal of Thermal Analysis and Calorimetry, 135, 763-786.

[28] Somalwal, K. (2017). A Review of Solar Collectors in Solar Thermal Applications. Int. J. Innov. Sci. Eng. Technol, 2, 23-27.

[29] Zhao, Z., Bai, F., Zhang, X., & Wang, Z. (2020). Experimental study of pin finned receiver tubes for a parabolic trough solar air collector. Solar Energy, 207, 91-102, https://doi.org/10.1016/j.solener.2020.06.070

[30] Nasir, A. (2004). Design, construction and experimental study of the thermal performance of a parabolic cylindrical trough solar air heater. AU Journal of Technology, 8(1), 21-26.

[31] Pandey, S., Mishra, S. K., Sharma, A., Verma, A. K., & Yadav, L. (2022). Performance analysis of evacuated tube type solar air heater with parabolic trough type collector. International Journal of Energy and Water Resources, 6(3), 337-351.https://doi.org/10.1007/s42108-021-00158-w

[32] Wang, P. Y., Guan, H. Y., Liu, Z. H., Wang, G. S., Zhao, F., & Xiao, H. S. (2014). High temperature collecting performance of a new all-glass evacuated tubular solar air heater with U-shaped tube heat exchanger. Energy Conversion and Management, 77, 315-323. https://doi.org/10.1016/j.enconman.2013.08.019.

[33] Good, P., Zanganeh, G., Ambrosetti, G., Barbato, M. C., Pedretti, A., & Steinfeld, A. (2014). Towards a commercial parabolic trough CSP system using air as heat transfer fluid. Energy Procedia, 49, 381-385. https://doi.org/10.1016/j.egypro.2014.03.041.

[34] Al-Sulaiman, F. A., Zubair, M. I., Atif, M., Gandhidasan, P., Al-Dini, S. A., & Antar, M. A. (2015). Humidification dehumidification desalination system using parabolic trough solar air collector. Applied Thermal Engineering, 75, 809-816. https://doi.org/10.1016/j.applthermaleng.2014.10.072

[35] Karoua, H., Debbache, M., Takilalte, A., Mahfoud, O., Moummi, A., Moummi, N., & Aoues, K. (2016, November). An experimental study of a new Solar Air Heater with a Linear Fresnel Reflector. In 2016 International Renewable and Sustainable Energy Conference (IRSEC) (pp. 104-108). IEEE.

[36] Hongfei Zheng , Tao Tao, Ming Ma, Huifang Kang, Yuehong Su (2012). Experimental test of a novel multi-surface trough solar concentrator for air heating. Energy Conversion and Management. https://doi.org/10.1016/j.enconman.2012.01.034

[37] Chu, S., Bai, F., Zhang, X., Yang, B., Cui, Z., & Nie, F. (2018). Experimental study and thermal analysis of a tubular pressurized air receiver. Renewable energy, 125, 413-424. https://doi.org/10.1016/j.renene.2018.02.125.

[38] Laouini, A., Benhaoua, B., Aoues, K., & Atia, A. (2021, February). Realization of a Solar Dryer Assisted by a Parabolic Dish Concentrator. In Defect and Diffusion Forum (Vol. 406, pp. 192-199). Trans Tech Publications Ltd, https://doi.org/10.4028/www.scientific.net/DDF.406.192.

[39] Khan, M. A., Rahman, M., Hanif, M., & Shah, S. F. (2013). Development of a small scale concentrating parabolic trough solar collector for drying purposes. Fahad, Development of a Small Scale Concentrating Parabolic Trough Solar Collector for Drying Purposes .

[40] F. Ullah, F., & Kang, M. (2017). Impact of air flow rate on drying of apples and performance assessment of parabolic trough solar collector. Applied Thermal Engineering, 127, 275-280 https://doi.org/10.1016/j.applthermaleng.2017.07.101.

[41] Ullah, F., Mansoor, K. K., Khan, M., Hassan, L., & Hasrat, K. (2016). Impact of the dehydration process on guava by using of the parabolic trough solar concentrator. Pakistan J Food Sci, 26(2), 92-7.

[42] El-Sebaii, A. A., Aboul-Enein, S., Ramadan, M. R. I., & El-Gohary, H. G. (2002). Experimental investigation of an indirect type natural convection solar dryer. Energy conversion and management, 43(16), 2251-2266. https://doi.org/10.1016/S0196-8904(01)00152-2.

[43] Enibe, S. O. (2002). Performance of a natural circulation solar air heating system with phase change material energy storage. Renewable Energy, 27(1), 69-86. https://doi.org/10.1016/S0960-1481 (01)00173-2

[44] Esakkimuthu, S., Hassabou, A. H., Palaniappan, C., Spinnler, M., Blumenberg, J., & Velraj, R. (2013). Experimental investigation on phase change material based thermal storage system for solar air heating applications. Solar Energy, 88, 144-153. https://doi.org/10.1016/j.solener.2012.11.006.

[45] Shalaby, S. M., & Bek, M. A. (2014). Experimental investigation of a novel indirect solar dryer implementing PCM as energy storage medium. Energy conversion and management, 83, 1-8. https://doi.org/10.1016/j.enconman.2014.03.043.

[46] Jain, D., & Tewari, P. (2015). Performance of indirect through pass natural convective solar crop dryer with phase change thermal energy storage. Renewable energy, 80, 244-250. https://doi.org/10.1016/j.renene.2015.02.012

[47] Dina, S. F., Ambarita, H., Napitupulu, F. H., & Kawai, H. (2015). Study on effectiveness of continuous solar dryer integrated with desiccant thermal storage for drying cocoa beans. Case Studies in Thermal Engineering, 5, 32-40. https://doi.org/10.1016/j.csite.2014.11.003.

[48] Shringi, V., Kothari, S., & Panwar, N. L. (2014). Experimental investigation of drying of garlic clove in solar dryer using phase change material as energy storage. Journal of Thermal Analysis and Calorimetry, 118(1), 533-539. https://doi.org/10.1007/s10973-014-3991-0

[49] El Khadraoui, A., Bouadila, S., Kooli, S., Farhat, A., & Guizani, A. (2017). Thermal behavior of indirect solar dryer: Nocturnal usage of solar air collector with PCM. Journal of cleaner production, 148, 37-48. https://doi.org/10.1016/j.jclepro.2017.01.149.

[50] Ramirez, C., Palacio, M., & Carmona, M. (2020). Reduced model and comparative analysis of the thermal performance of indirect solar dryer with and without PCM. Energies, 13(20), 5508. https://doi.org/10.3390/en13205508.

[51] Vijayan, S., Arjunan, T. V., & Kumar, A. (2020). Exergo-environmental analysis of an indirect forced convection solar dryer for drying bitter gourd slices. Renewable Energy, 146, 2210-2223. https://doi.org/10.1016/j.renene.2019.08.066.

[52] Bhardwaj, A. K., Kumar, R., Chauhan, R., & Kumar, S. (2020). Experimental investigation and performance evaluation of a novel solar dryer integrated with a combination of SHS and PCM for drying chilli in the Himalayan region. Thermal Science and Engineering Progress, 20, 100713. https://doi.org/10.1016/j.tsep.2020.100713.

[53] Moghimi, P., Rahimzadeh, H., & Ahmadpour, A. (2021). Experimental and numerical optimal design of a household solar fruit and vegetable dryer. Solar Energy, 214, 575-587. https://doi.org/10.1016/j.solener.2020.12.023.

[54] AA, A. A., Omara, A. A., Ahmed, E. K., Babiker, R. M., & Mohammedali, A. A. (2021, February). Experimental Study on Tomato Drying Using a Solar Dryer Integrated with Reflectors and Phase Change Material. In 2020 International Conference on Computer, Control, Electrical, and Electronics Engineering (ICCCEEE) (pp. 1-5). IEEE.

[55] Saikia, D., Nayak, P. K., Sivakumaranb, N., Kondareddy, R., Krishnan, K. R., & Dutta, J. (2022). Latent heat storage system based mixed mode indirect solar dryer for drying myrobalan. https://doi.org/10.21272/jnep.14(3).03022.

[56] Bareen, A., Dash, S., Kalita, P., & Dash, K. K. (2024). Experimental investigation of an indirect solar dryer with PCM-integrated solar collector as a thermal energy storage medium. Environmental Science and Pollution Research, 31(12), 18209-18225. https://doi.org/10.1007/s11356-023-26690-2.

[57] Chaatouf, D., Raillani, B., Salhi, M., Amraqui, S., & Mezrhab, A. (2023). Experimental and numerical study of a natural convection indirect solar dryer with PCM tubes: Dynamic, thermal and nutritional quality analysis. Solar Energy, 264, 111975. https://doi.org/10.1016/j.solener.2023.111975.

[58] Bousbia Salah, S. E., Benseddik, A., Meneceur, N., Zine, A., & Deghoum, K. (2024). Design and realization of a new solar dryer assisted by a parabolic trough concentrator (PTC) with a dual-axis solar tracker. Solar Energy, 283, 113001. https://doi.org/10.1016/j.solener.2024.113001

[59] J.A. Duffie, W.A. Beckman, Solar Engineering of Thermal Processes, second ed., Wiley Interscience, New York, 1991. pp. 358–361

[60] Kalogirou. S.A., Solar thermal collectors and applications, Prog. Energy Combust.Sci.30,(3).231–295.2004. https://doi.org/10.1016/j.pecs.2004.02.001.these

[61] Zarza Moya, E. 2012. Parabolic trough concentrating solar power (CSP) systems, Chapter 7. In Concentrating Solar Power Technology: Principles, Developments and Applications, K. Lovegrove, and W. Stein eds. Woodhead Publishing Lt., Cambridge, UK.

[62] Kedwards D., Marlot L., Capteurs Solaires, Edition S C M, Paris (1979).

[63] Steinfeld A. et Palumbo R., Solar thermochemical process technology. Encyclopedia of physical science et technology 15, 237-256 (2001).

[64] K. F. Yogi D.G, Kreider J.F, (1999) Off-Normal Incidence Effects, in Principles of solar engineering, T. Francis., Ed., 2nd Edition ed, pp. 139.

[65] S. Kalogirou, S. Lloyd and J. Ward, 'A Simplified Method for Estimating Intercept Factor of Parabolic Through Collectors', Proceedings of the Forth Word Renewable Energy Congress, Denver, Colorado, USA, Vol. 3, pp. 1782 – 1786, 1996.

[66] J.A. Duffie, W.A. Beckman, Solar Engineering of Thermal Processes, Hoboken, John Wiley & Sons, New Jersey, 1991.

[67] Shitzer, A. (2006). Wind-chill-equivalent temperatures: regarding the impact due to the variability of the environmental convective heat transfer coefficient. International journal of biometeorology, 50, 224-232. https://doi.org/10.1007/s00484-005-0011-x

[68] Zografos, A. I., Martin, W. A., & Sunderland, J. E. (1987). Equations of properties as a function of temperature for seven fluids. Computer Methods in Applied Mechanics and Engineering, 61(2), 177-187. https://doi.org/10.1016/0045-7825(87)90003-X

[69] Benseddik, A., Azzi, A., Zidoune, M. N., Khanniche, R., & Besombes, C. (2019). Empirical and diffusion models of rehydration process of differently dried pumpkin slices. Journal of the Saudi Society of Agricultural Sciences, 18(4), 401-410. https://doi.org/10.1016/j.jssas.2018.01.003

[70] Benseddik, A., Azzi, A., & Allaf, K. (2018). Mathematical empirical models of thin-layer airflow drying kinetics of pumpkin slice. Engineering in Agriculture, Environment and Food, 11(4), 220-231. https://doi.org/10.1016/j.eaef.2018.07.003

[71] J. Crank, The Mathematics of Diffusion. 2nd Edition, Oxford University Press, London 1975.

[72] Selvanayaki, S., & Sampathkumar, K. (2017). Techno-economic analysis of solar dryers. In Solar drying technology: concept, design, testing, modeling, economics, and environment (pp. 463-493). Singapore: Springer Singapore. https://doi.org/10.1007/978-981-10-3833-4_16

[73] Kherrafi, M. A., Benseddik, A., Saim, R., Bouregueba, A., Badji, A., Nettari, C., ... & Bensaha, H. (2023). Performance enhancement of indirect solar dryer with offset strip fins: Experimental investigation and comparative analysis. Solar Energy, 266, 112158. https://doi.org/10.1016/j.solener.2023.112158

[74] Weather Spark. Available online: https://weatherspark.com/y/53031/Average-Weather-in-El-Oued-Algeria-Year-Round#Sections-Clouds (accessed on December 2022).

[75] Climates to travel, World climate guide. Available online: https://www.climatestotravel.com /climate/algeria/el-oued (accessed on December 2022).

[76] NASA power prediction of worldwide energy resources Available online: https:// power.larc.nasa.gov/data-access-viewer/ (accessed on December 2022).

[77] Solargis. Global Solar Atlas n.d. Available online: https://globalsolaratlas.info/download/algeria (accessed on December 2022).

[78] Gaisma. Available online: https://www.gaisma.com/en/location/el-oued.html (accessed on December 2022).

[79] PD: 3D Sun-Path. An app to model the orbital relationship between the Earth and the Sun. Available online: https://drajmarsh.bitbucket.io/earthsun.html. (Accessed on June 2023).

[80] Sun Earth Tools. Tools for consumers and designers of solar. Available online: https://www.sunearthtools.com/dp/tools/pos_sun.php#top. (Accessed on June 2023).

[81] Google Earth Engine. Available online: https://earth.google.com/web/ @33.31530616, 6.78358367, 97.28189243a, 13423.83511848d,35y,0h,0t,0r (accessed on February 2025)

[82] Hadeid, M., Ghodbani, T., Dari, O., & Bellal, S. A. (2021). Saharan Agriculture in the Algerian Oasis: Limited Adaptation to Environmental, Social and Economic Changes. *Climate Change and Water Resources in Africa: Perspectives and Solutions Towards an Imminent Water Crisis*, 239-253. https://doi.org/10.1007/978-3-030-61225-2_11

[83] Berbache, H., Khaoui, M., & Hadjab, M. (2022). The oasis system in southern Algeria: a natural heritage threatened with disappearance, case of the oasis of Biskra. *Technium Soc. Sci. J.*, *34*, 588.

[84] Li, X., Yang, K., & Zhou, Y. (2016). Progress in the study of oasis-desert interactions. *Agricultural and Forest Meteorology*, *230*, 1-7. https://doi.org/10.1016/j.agrformet.2016.08.022

[85] NMO. National Meteorological Office. Available online: https://www.meteo.dz/ (accessed on Jun 2023).

[86] Nettari, C., Boubekri, A., Benseddik, A., Bouhoun, S., Daoud, D., Badji, A., & Hasrane, I. (2024). Design and performance evaluation of an innovative medium-scale solar dryer with heat recovery based-latent heat storage: Experimental and mathematical analysis of tomato drying. Journal of Energy Storage, 88, 111559. https://doi.org/10.1016/j.est.2024.111559

[87] Rubitherm Technologies GmbH. Available online: https:// www.rubitherm.eu /en/ productcategory/ organische - pcm-rt (accessed on February 2025)

[88] Kumar, S. K., Muniamuthu, S., Mohan, A., Amirthalingam, P., & Anbu Muthuraja, M. (2022). Effect of Charging and Discharging Process of PCM with Paraffin and Al_2O_3 Additive Subjected to Three Point Temperature Locations. Journal of Ecological Engineering, 23(2), 34-42

[89] Senthil, R., Patel, A., Rao, R., & Ganeriwal, S. (2020). Melting behavior of phase change material in a solar vertical thermal energy storage with variable length fins added on the heat transfer tube surfaces. International Journal of Renewable Energy Development, 9(3), 361.

[90] FAO. FAO Statistical Database. 2023. Available online: https:// www.fao.org/faostat/en/#data/QCL, (accessed on February 2025).

[91] Boutiti, K., Belil, I., & Khelifi, D. (2018). Characterization of Algerian apricots (Prunus armeniaca) using morphological and pomological markers. *Int J Modern Science*, *8*, 631-639.

[92] Mukama, M., Ambaw, A., & Opara, U. L. (2020). Thermophysical properties of fruit—a review with reference to postharvest handling. *Journal of Food Measurement and Characterization*, *14*, 2917-2937. https://doi.org/10.1007/s11694-020-00536-8

[93] Muhlbauer, W., & Muller, J. (2020). *Drying atlas: Drying kinetics and quality of agricultural products*. Woodhead Publishing.

[94] Yang, Q., Yi, X., Xiao, H., Wang, X., Liu, L., Tang, Z., Hu, C., & Li, X. (2024). Effects of Different Drying Methods on Drying Characteristics, Microstructure, Quality, and Energy Consumption of Apricot Slices. *Foods*, *13*(9), 1295. https://doi.org/10.3390/foods13091295

[95] Satorabi, M., Salehi, F., & Rasouli, M. (2021). The Effect of Gum Based Edible Coating on the Infrared Drying Performance of Apricot Slices. *Journal of Food Biosciences and Technology, 11(2), 1-10. SID*

Appendices

Appendices

Appendix A: List of used software

	Software	Information
1	**MATLAB**	Is a proprietary programming language and numerical computing environment developed by *MathWorks*. It is widely used for matrix operations, simulations, data analysis, and algorithm development.
2	**Parabola calculator**	Is a software tool that computes key properties of a parabola, such as its vertex, focus, axis of symmetry, and intercepts.
3	**SOLIDWORKS**	Is a professional 3d cad software used for designing, simulating, and analyzing mechanical products and systems.
4	**VOS VIEWER**	Is a software tool used for creating and visualizing Bibliometric networks
5	**ORIGIN**	Is a software application used for data analysis and scientific graphing, widely employed in research and engineering fields
6	**EXCEL**	Is the industry-leading spreadsheet program and a powerful tool for data visualization and analysis.

Appendix B: Scientific Achievements

- **Publications**
  1. **1.** Bousbia Salah, S. E., Benseddik, A., Meneceur, N., Zine, A., & Deghoum, K. (2024). Design and realization of a new solar dryer assisted by a parabolic trough concentrator (PTC) with a dual-axis solar tracker. *Solar Energy*, *283*, 113001.

Solar Energy 283 (2024) 113001

Contents lists available at ScienceDirect

Solar Energy

journal homepage: www.elsevier.com/locate/solener

Design and realization of a new solar dryer assisted by a parabolic trough concentrator (PTC) with a dual-axis solar tracker

Seif Eddine Bousbia Salah [a], Abdelouahab Benseddik [b,*], Noureddine Meneceur [a], Ali Zine [a], Khalil Deghoum [a]

[a] UDERZA Unit, Faculty of Technology, University of El Oued, 39000 El Oued, Algeria
[b] Unité de Recherche Appliquée en Energies Renouvelables, URAER, Centre de Développement des Energies Renouvelables, CDER, 47133 Ghardaïa, Algeria

ARTICLE INFO

Keywords:
Solar drying
Parabolic trough concentrator (PTC)
Solar tracking system
Heat transfer fluid (HTF)
Apricot

ABSTRACT

This article presents the design, fabrication, and testing of a new solar dryer equipped with a tracking system. The dryer was assisted by a cylindrical-parabolic concentrator which moved along two vertical and horizontal axes. The study was conducted at El-Oued University (latitude 33°23′N and longitude 6°51′E). The experimental performance evaluation involved drying 10 kg of apricots from 69 % to 8 % moisture content (wb). The thermal efficiency of the dryer was tested under no-load and full-load conditions. The results indicated that the solar dryer achieved a temperature of up to 115 °C at the receiver in the focal line and 70 °C in the drying chamber, which was sufficient for effective drying of various agricultural products. Additionally, an economic analysis further substantiates the viability of our solar dryer, showcasing a notably low capital cost and negligible electricity expenses. With a substantial difference in the cost of fresh versus dried apricots, our system boasts a reduced payback period estimated at 0.43 years. This research demonstrates the potential of using solar power to dry crops and reduce dependence on fossil fuels.

1. Introduction

Solar energy is one of the most promising energy sources for

are based on numerical simulations, while others are based on experimental results. So, most research focused their work on the reduction of losses and the improvement of the heat transfer between the receiving tube and the heat transfer fluid by using thermal oil, water, air, nanofluid, etc. However, its applications were limited to the field of hot air

- **Communications**

1. **Bousbia Salah, S. E**., Benseddik, A., & Meneceur, N. (2024, November 13-14). *Enhancing the efficiency of an indirect solar dryer integrating sand and coal as thermal energy storage* [Conference presentation]. 1st International Conference on Renewable Energy Applications in Agriculture (ICREAA-2024), Ghardaïa, Algeria.

2.

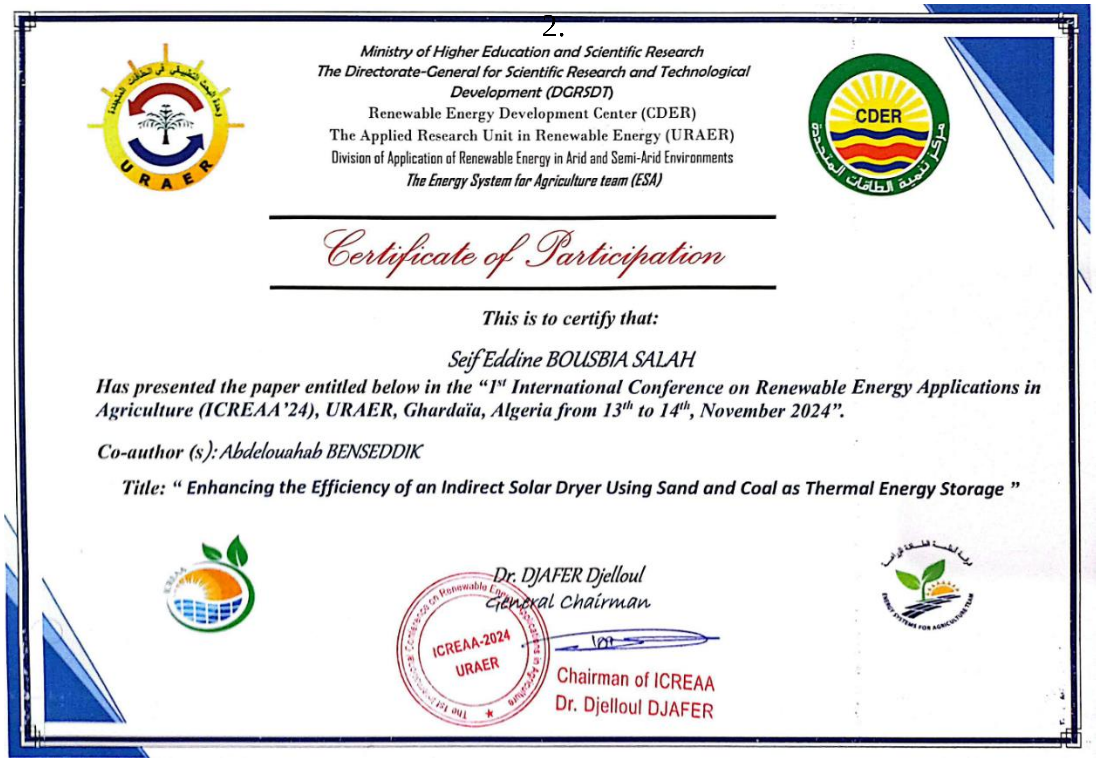

2. Messaoud, Z., **Bousbia, S. E**., Benseid, A., Aldaoul, L. (2023, *Month*). *Modélisation de la cinétique de séchage en couche mince des pommes de terre dans un séchoir solaire direct à convection forcée* [Poster presentation]. 1st International Conference for Renewable Energies and Their Applications (1st ICERA-2023), *Conference Location*.


Unité de Recherche Appliquée en Energies Renouvelables URAER
Division Applications des énergies renouvelables dans les milieux arides et semi-arides
Equipe : Systèmes Energétiques pour l'Agricultures

Les Techniques et les Applications du séchage solaire

Attestation de Participation

La 1ere journée d'étude sur les Techniques et les Applications du Séchage Solaire, le 27 Octobre 2022 à Ghardaïa

Le président de la 1ere journée d'étude TASS' 2022 atteste que : *BOUSBIA Salah Seif Eddine*

Co-auteurs : *ZINE Ali*

A participé à la 1ere journée d'étude TASS' s'est déroulée le 27 octobre 2022 à Unité de Recherche Appliquée en Energies Renouvelables URAER, Ghardaïa par une présentation poster intitulée :

Séchage des produits agricoles locaux à l'aide d'un séchoir solaire dans la zone d'El-Oued

Le président de la journée


جامعة الشهيد حمه لخضر - الوادي
Echahid Hamma Lakhdar University- El Oued
وحدة البحث تطوير الطاقات المتجددة في المناطق القاحلة
Renewable Energy development unit in Arid Zones
كلية التكنولوجيا
Faculty of Technology

First International Conference for Renewable Energies and Their Applications (1st ICERA-2023)

Certificate of Participation

This is to certify that **Zelaci Messaoud** *presented a Poster presentation at the* 1st ICERA-2023

the paper entitled

Modélisation de la Cinétique de Séchage en Couche Mince des Pommes de Terre dans un Séchoir Solaire Direct à Convection Forcée

Co-Authors: Bousbia Salah seif Eddine, Benseddik abdelouahab, Aidaoui lakhdar, Zine ali

1st ICERA-2023 General Chair